Dollas of 2

RETURN TO INSTRUMENT
BRANCH FILE

/NF. 217C-7

NACA

CLASSIFICATION CHANGED
To *Unclassified*
By authority of *naca Research*
Abstract no 56 Date 1/18/57

RESEARCH MEMORANDUM

EXPERIMENTAL INVESTIGATION OF AIR-COOLED

TURBINE BLADES IN TURBOJET ENGINE

I- ROTOR BLADES WITH 10 TUBES IN

COOLING-AIR PASSAGES

By Herman H. Ellerbrock
and Francis S. Stepka

Lewis Flight Propulsion Laboratory
Cleveland, Ohio

RETURN TO INSTRUMENT
BRANCH FILE

NATIONAL ADVISORY COMMITTEE
FOR AERONAUTICS
WASHINGTON

CLASSIFICATION CHANGED
To *Unclassified*
By authority of *naca Research*
Abstract no. 56 Date 4/1/57

2/11/56

1410

NATIONAL ADVISORY COMMITTEE FOR AERONAUTICS

RESEARCH MEMORANDUM

EXPERIMENTAL INVESTIGATION OF AIR-COOLED

TURBINE BLADES IN TURBOJET ENGINE

I - ROTOR BLADES WITH 10 TUBES IN

COOLING-AIR PASSAGES

By Herman H. Ellerbrock, Jr.
and Francis S. Stepka

SUMMARY

An investigation is being conducted to determine experimentally
the effectiveness of air cooling several turbine-blade configura-
tions in a turbojet engine. The results obtained with the first
configuration, a hollow blade shell with 10 tube inserts, are
presented.

A production turbojet engine was modified and instrumented
for the investigation. Two of the original turbine blades, which
were located diametrically opposite in the rotor, were replaced by
untwisted air-cooled hollow blades. In order to decrease unfavor-
able flow conditions that would arise from having untwisted hollow
blades located between two of the original twisted blades, two of
the original blades on the concave side and one on the convex side
of the hollow blades were removed and replaced by solid untwisted
blades that had the same outside contour as the hollow blades.
The investigation determined the radial temperature distribution
along the trailing edge and the peripheral temperature distribution
at approximately one-third of the blade span from the blade base
of a cooled blade. The cooling-air-flow rate per blade varied
from 0.004 to 0.175 pound per second during the investigation. The
rotor speed varied from 4000 to 10,500 rpm and the gas-flow rate
from 18.8 to 61.5 pounds per second.

The results indicated appreciable cooling of the blade at the
midchord but the leading and trailing edges were much hotter. For
example, at an engine speed of 10,000 rpm, a cooling-air tempera-
ture at the blade root of 100° F, and a cooling-air-flow rate per
blade about 6 percent of the engine gas-flow rate per blade,
trailing-edge, leading-edge, and midchord temperatures were

about 790°, 760°, and 470° F, respectively, as compared with about
960° F for the uncooled blade. The temperature data for most
thermocouple positions were correlated for the conditions investi-
gated through use of a parameter indicated by theory. Such cor-
relations are required for comparisons of blade configurations at
the same engine and cooling-air conditions and for predicting cool-
ing effectiveness for any conditions. A method of calculating
solid-blade temperatures, which are equal to the gas temperatures
effecting heat transfer, was developed; the method gave values
that deviated not more than 20° F from the measured temperatures.
Such temperatures are required for predicting cooled-blade tempera-
tures from the correlations.

INTRODUCTION

The primary objectives of turbine cooling are to obtain blade
configurations, made of nonstrategic metals, that can be adequately
cooled at currently encountered gas temperatures, and to extend
the operating range of turbines to higher gas temperatures using
the same metals if possible. In order to arrive at these objec-
tives, several phases of experimental and analytical research must
be simultaneously conducted. Essentially, the work is concerned
with the theoretical and experimental determination of heat-
transfer coefficients, the theory of blade-temperature distribu-
tion and coolant-flow requirements, the experimental investigations
of cooled turbines, and the analysis of the effects of cooling on
engine operation and performance.

Investigations have been made to determine the gas-to-blade
heat-transfer coefficients and their laws for several different
blade shapes in static cascades (reference 1) and in a turbine
(reference 2). Additional investigations have been made on air-
cooled blades in order to determine the blade-to-coolant heat-
transfer coefficients for hollow blades and hollow blades with
fins in the cooling-air passages. Equations have been developed
for the determination of blade-temperature distribution in air-
cooled blades with normal forced-convection cooling (reference 3)
and of the cooling-air-flow characteristics in the blade passages
(reference 4).

These data and equations, with other material, have been used
to predict analytically the effect of air cooling turbine blades,
which have various internal configurations, on the turbine-inlet
temperature or the power of typical turbojet and turbine-propeller
engines. Some results are given in references 5 and 6. The

1410

experimental investigations of blades in cascades and the analyses
of engine cycles indicate that some configuration other than the
hollow blade must be used if adequate cooling is to be obtained.
The most promising configurations were hollow blades with metal
inserts such as tubes or fins that would increase the internal
heat-transfer area and thus provide better blade cooling.

Experiments and calculations indicate that the leading and
trailing edges of the blades are the most difficult portions to
cool and that the temperatures of these parts rapidly increase as
the distance from the coolant increases. Calculations (refer-
ence 7) show that this distance should be limited to about
1/4 inch in order that the trailing-edge temperatures be about the
same as the midchord temperatures. Experiments on finned blades
in cascades and on water-cooled blades (reference 2) show high
trailing-edge temperatures. In order to realize the improvements
theoretically obtainable by air-cooling turbine blades, the research
to date therefore indicates that special means of cooling the lead-
ing and trailing edges must be used.

Tests on a cascade of blades (reference 8) have been made
where "chevron" slots in the leading edge and small slots
(0.005 in. wide) in the trailing edge have been used with success
for cooling these parts. The cooling air passed from the inside
to the outside of the blade through the slots and formed a cool
layer of air between the gas and the blade. Another type of slot
used for film cooling was investigated in a cascade of blades (ref-
erence 9) with radial slots in the blade shell at various positions
along the surface. These investigations indicate that beneficial
cooling effects at the slot position and immediately downstream of
the slot can be obtained.

With this background knowledge available for choosing blade
configurations, an investigation was started at the NACA Lewis lab-
oratory in November 1949 to verify the experimental effectiveness
of various air-cooled blade configurations when used in a typical
turbojet engine. The primary objective of the investigation is to
obtain configurations that allow the engine to operate at current
gas temperature using nonstrategic materials for blades. The sec-
ondary objective is to obtain configurations that will allow use
of such materials and also permit the use of higher turbine-inlet
temperatures.

The cooling data obtained with the first blade configuration
installed in the engine are presented herein. The rotor of this
engine was altered by removing several of the conventional blades

1410

and replacing them with experimental blades. For this study, adequate data were obtained by using only two cooled blades, which were instrumented to provide readings of the radial distribution of temperature along the trailing edge and the peripheral-blade-temperature distribution at a distance of about one-third of the blade span from the base. The cooled blades had 10 tubes inserted in the hollow core to increase the internal heat-transfer surface. A simple blade with no special leading- and trailing-edge cooling arrangements was used in this first study in order to determine how effective a blade would be that could be easily manufactured. For aerodynamic reasons, additional uncooled blades of the same profile as the cooled blades were placed on either side of the cooled blades so as to provide two rotating cascades of four blades each at diametrically opposite positions on the turbine wheel. A thermocouple was placed near the leading edge of one uncooled blade next to each air-cooled blade to obtain a reference temperature. Cooling air was supplied to each air-cooled blade through a modified tail cone. In order to determine the effect of operating conditions on blade temperatures, experiments were conducted at several constant engine speeds from 4000 to 10,500 rpm over a range of cooling-air flows from about 2 to 50 percent of the combustion-gas flows.

Mr. Roger Long of this laboratory was responsible for developing the techniques and guiding the fabrication of the blades used in the investigation.

APPARATUS

In order to establish an experimental comparison between cooled and uncooled turbine-blade temperatures in an actual operating engine, a commercial turbojet engine was modified and instrumented. The engine used had a dual-entry centrifugal compressor, a combustion-chamber assembly consisting of 14 individual burners, and a single-stage turbine.

General Engine Modifications

Blading modifications. - Two of the original turbine blades at diametrically opposite locations in the rotor were replaced by untwisted hollow blades, which were fitted with tube inserts. A view of the modified rotor is shown in figure 1.

In order to decrease the unfavorable flow conditions that may arise by having the untwisted hollow blades located between two of

the original twisted-type blades, which have a much greater taper than the modified hollow blades, two of the original blades on the concave side and one on the convex side of the hollow blades were removed and replaced by solid untwisted blades that had the same outside contour as the hollow blades (fig. 1). A close-up view of one set of modified blades mounted on the rotor is given in figure 2.

Cooling-air supply system. - Bleeding compressor air to cool the two hollow blades would have required extensive modification of the engine ducting; controlled air flow over a wide range of cooling-air-flow to gas-flow ratios was also desirable. An independent air supply was therefore used.

Blade cooling air was ducted into the modified tail cone through two 0.62-inch inside-diameter tubes (fig. 3), which were attached to a single 1-inch inside-diameter inlet tube that was concentric with and on the center line of the turbine rotor. The air then entered a housing attached to the rotor that served as an air chamber and bearing housing, as shown in figure 3. A labyrinth seal between the rotating housing and the cooling-air inlet tube kept leakage of the blade-cooling air to a negligible value. The end of the inlet tube that entered the air chamber was supported and alined by a pilot bearing in the housing; whereas the other end was supported by a flange having an adjustable connection that permitted small misalinements of this end of the tube with the pilot bearing.

An air-inlet guide plate (fig. 3) was located in the air-chamber housing, which divided and guided the air to the blades. This plate had two rectangular passages, which increased in depth with plate diameter. From the passages in this plate, the air entered two radial 1/2-inch inside-diameter stainless-steel tubes that were welded to the face of the rotor (figs. 1 and 3). The end of each tube near the rim of the turbine disk was welded into a hole in the disk. These holes were drilled upward from the downstream face of the rotor to the bottom of serrated grooves, which held the blades. At the bottom of each groove a slot was machined, which extended to the drilled hole and thus provided a smooth coolant passage to the blades. (This hole and slot arrangement is shown in fig. 3.) The angle at which the hole was drilled in the rotor was determined by studies that are described later.

The two inlet tubes through which cooling air was ducted into the tail cone were enclosed by concentric scavenge-air tubes through which secondary air was passed (fig. 3). The secondary

1410

air flow minimized the rise in temperature of the blade-cooling
air as it was piped through the tail-cone assembly. The air,
after flowing through these scavenge air tubes, was circulated
about the inner exhaust cone in order to ventilate and to scavenge
it of combustion gases. The scavenge air then passed into the
main gas stream through the clearance space between the rotor and
the inner cone. Because the pilot bearing in the air-chamber bear-
ing housing was operating under fairly high temperature conditions,
a tube was installed in the tail cone for the purpose of directing
a jet of cool air to the bearing (fig. 3).

The air supply for the blade-cooling air and the scavenge and
bearing-cooling air was bled from the main supply line. Pressure
regulating valves were installed in the line to dampen any line
fluctuations and to maintain a constant upstream pressure. Manu-
ally operated valves were installed downstream of the pressure
regulating valves to regulate the air flow.

Detail Description of Modified Blading

General construction. - The two cooled and six uncooled,
untwisted blade sections were cast and then welded to serrated
bases, which were cut from the conventional turbine blades
(fig. 4(a)). This method of fabrication was used in preference
to casting the blade and the base as an integral unit because of
the additional casting difficulties that would be encountered,
especially in the case of the hollow blades, and because of the
additional time that would be required to machine the serrated
grooves in the blade base.

Blade fabrication. - The hollow and solid modified blade sec-
tions were cast high-temperature alloy X-40 and the serrated base
material as obtained from the standard blades was cast high-
temperature alloy AMS 5385. The hollow blades were so cast that
the core area was constant over the length of the blade and the
outside wall tapered linearly from the root to the tip. The pro-
file of the cooled blade at its root was the same as that at the
root of the conventional blades used in the turbine. The nominal
thickness of the wall at the tip was 0.040 inch and at the base,
0.070 inch. In order to increase the internal heat-transfer sur-
face, 10 tubes were inserted in each hollow blade. They extended
through the blades from tip to base. These tubes were brazed to
each other and to the inside surface of the hollow blades. A com-
mercial brazing alloy was used, which is believed to have a strength
of approximately 90 percent of the blade material. Of the ten

tubes in each blade, four were 0.125-inch outside-diameter stainless-steel tubes with a wall thickness of 0.010 inch, and six were 0.156-inch outside-diameter low-carbon-steel tubes with a wall thickness of 0.0155 inch. The view of a cooled-blade tip (fig. 4(b)) illustrates the tube arrangement.

Because of the difficulties of drilling the cast-alloy base to provide the air-inlet slot that runs through this base to the core of the blade, the slot was burned out by an intermittent electric arc. The profile of this slot (fig. 4(c)) corresponds to that of the core of the hollow-blade section.

Instrumentation

Engine instrumentation. - The turbine rotor speed was measured by a chronometric tachometer and to aid the engine operator in keeping the speed constant a Stroboscopic tachometer was also used. The compressor-inlet air temperature was measured with shielded thermocouples, which were attached to the screens at the compressor inlet that prevent large particles of dirt or foreign matter from entering the engine. Three thermocouples were equally spaced circumferentially around both the front and the rear inlet screens. The compressor-outlet temperature and the total and static pressures were measured by probes located in the compressor-diffuser section just before the air enters the burners. The fuel flow was measured by rotameters.

In order to determine the mass flow of the engine, a pressure-temperature airfoil-type survey rake was installed in the tail pipe approximately 6 feet downstream of the turbine rotor, which is approximately 1 foot upstream of an adjustable exhaust nozzle located at the end of the tail pipe. Chromel-alumel thermocouples were used in the rake.

Coolant measurements. - A thermocouple was installed in the blade-cooling-air tube located on the engine center line to measure the temperature of the cooling air before it entered the air chamber at the hub of the rotor. Another thermocouple was attached in a groove on this tube at the section where the bearing is located to measure the pilot bearing temperature while the engine was in operation.

The blade cooling-air flow was controlled by manually operated valves. The flow was metered by standard flat-plate orifices. Two parallel-orifice runs were used, one for large flow rates and one for small flow rates.

1410

The bearing cooling and scavenge air were independently con-
trolled and the flow rates were metered together using a flat-
plate orifice.

Blade instrumentation. - Chromel-alumel thermocouples (num-
ber 36 wire) were installed on the two air-cooled blades (four on
each blade) and one thermocouple on each of the solid blades next
to the air-cooled blades. The locations of the thermocouples are
shown in the sketches of the blades in figure 5. The solid-blade
thermocouples (F and L) were located near the leading edge in
identical positions on each of the two blades. Four of the air-
cooled-blade thermocouples (A, B, C, and D) were located near the
trailing edge of one blade and the other four formed a band around
the other air-cooled blade. Three of these thermocouples (G, H,
and I) were located at the same distance from the root as the
solid-blade thermocouples and one thermocouple (J) was 3/16 inch
above the others in the band. Thermocouples I and C were approxi-
mately at the same positions on the two air-cooled blades; thermo-
couples G and L were also in corresponding positions (fig. 5).
This arrangement provided a reference between cooled- and uncooled-
blade temperatures and between temperatures of the two air-cooled
blades. A thermocouple was also placed in each cooling-air-inlet
passage near the blade root for measuring the cooling-air tempera-
ture at this position (thermocouples E and K, fig. 5).

The blade-thermocouple wire was insulated by two-hole ceramic
tubing, which was enclosed in 0.040-inch outside-diameter Inconel
tubes that were buried in grooves cut in the surface of the blades,
as shown in figures 4 and 6. After the leads were in place, the
grooves were brazed over with a commercial brazing alloy, which
after finishing left the blade surface smooth.

Thermocouples E and K (fig. 5) were insulated from the passage
walls and were located in the passage at the point where the
radial cooling-air-inlet tube bends and enters the hole in the
face of the wheel. The thermocouple leads emerging from the tube
at this point are shown in figure 1. From this point these leads,
as well as the blade-thermocouple leads, were run along the face
of the wheel toward the hub where they were connected to insulated
points on a junction ring. From this ring, 12 pairs of chromel-
alumel wires were run in grooves in the air-inlet guide plate and
then through the drilled turbine and compressor shaft to the front
of the engine, where they were connected to a slip-ring-type ther-
mocouple pickup, shown in figure 7. Because only six thermocouples
could be read at one time with the slip-ring assembly, a bakelite

terminal coupling (fig. 7) was used, which by having jumper con-
nections across the terminal screws permitted the reading of any
combination of six of the thermocouples. As a consequence, tests
were conducted first with the thermocouple combination A, B, C, D,
E, and F and then repeated with the combination G, H, I, J, K, and L.

STUDIES LEADING TO DESIGNS

As a result of marked differences between this engine modifi-
cation and the type of apparatus previously used for cooled tur-
bine research, a number of preliminary design studies were con-
ducted to determine the suitability of the configurations selected
and any limitations that might occur in operation.

Turbine Modifications

Cooling-air radial-inlet passages. - The cooling-air radial-
inlet-passage arrangement shown in figure 3 appeared to be the
simplest means available. The passages were exposed to heating by
conduction from the turbine wheel and by convection from the region
inside the inner exhaust cone with consequent possible limitations
in the coolant weight flow and the supply temperature that could
be maintained at the blade base. The diameter of these passages
was limited to 1/2-inch inside diameter by stress considerations
in the turbine rim and blade-root serration. Complete stress anal-
ysis could not be made in the time available, but removal of more
metal than required by the 1/2-inch inside-diameter tube did not
appear reasonable. The possibility of attaching the tube to the
wheel by means of straps was considered because this arrangement
would permit insulation between the tube and the wheel, but stress
analysis showed that it was necessary to weld the tube to the wheel
throughout its length. Preliminary calculations were made to check
the cooling-air temperature rise and the Mach numbers in the pas-
sages; it was found that temperature rise was not a limitation.
The excess cooling air supplied to the inner exhaust cone results
in lower temperatures at the face of the turbine wheel than would
be encountered in normal operation. The flow conditions were ana-
lytically determined at the blade tip where sonic Mach number is
first reached, and the Mach number in the radial passage was
always considerably below that in the blade passage.

In this investigation, an external source of cooling air was
provided; therefore, entrance losses and pressure drops in the sup-
ply system to the blade base were unimportant. A bench test was

made in a mock-up of the design, however, to check the effect of
the angular entrance at the blade base on the distribution of cool-
ing air in the blade passages. The test was actually made with a
finned blade, which may react differently from the tubes used in
the blades in the engine, but the results indicated a uniform flow
distribution except in the portions of the coolant passage near
the leading and trailing edges when the air entered the base at a
45° angle with the horizontal. The general effect of heat trans-
fer to the cooling air in the blade during actual operation is to
increase the static pressure and to reduce the entrance velocity
at the base of the blade, therefore the effect of entrance angle
on flow distribution would be even less in the engine.

Coolant-flow limitations. - Preliminary calculations indi-
cated that the coolant passage would choke at the blade tip and
limit the coolant-flow to the order of 10 percent of the engine
weight flow at rated speed when all rotor blades are assumed to be
cooled. The external supply source, however, permitted increase
in coolant flow ratio beyond the original choking value simply by
increasing the static pressure and the density of the coolant
throughout the cooling system. The remaining limitations that
required further investigation were the effect of tip clearance on
the coolant weight flow and the possibility of interference effects
between the jet emerging from the turbine nozzles and the jet
emerging from the blade tip. Further bench tests were made to
obtain at least a qualitative interpretation of these effects by
use of the apparatus illustrated in figure 8.

A single cooled-type blade was installed in tandem with four
standard uncooled-type blades in a segment of a rotor disk. The
cooled-type blade was the same in all respects as the air-cooled
blade used in the engine as previously described except that it
had fins inside the blade shell rather than tubes. The finned
blade was used in order to expedite the experiment because tubed
blades were unavailable at the time. The orientation of the blade
with respect to the blade base was similar to that designed for
the full-scale turbine. A series of static-pressure orifices was
installed in the coolant passage at a distance of 1/32 inch from
the blade tip.

Coolant, supplied by the laboratory-service air system, was
passed through a pressure regulator, which dampened the pressure
fluctuations. After passing through the orifice run, the coolant
was directed to the root of the hollow test blade through a pas-
sage configuration that duplicated the configuration designed for
the full-scale-turbine installation. Total and static pressures

of the coolant were obtained in the coolant supply tube at a station immediately upstream of the coolant-passage transition section in the blade base.

A means was provided for simulating the flow in the clearance space across the blade tip, as occasioned by the flow out of the turbine nozzles. The device consisted of an air jet directed across the open end of the cooled blade beneath a curved sheet-metal plate, which served to simulate the stationary turbine-blade shroud (fig. 8). The jet flow was directed across the blade tip at an angle corresponding to the calculated angle of the relative velocity at the tip section at the rotor inlet. The axial clearance between the jet discharge and the leading edge of the blade tip was fixed at 7/8 inch (same as for the cooled blade in the full-scale engine). Although a jet velocity of Mach number $M = 1.0$ was desired, the maximum velocity obtainable with the apparatus was about $M = 0.65$ (630 ft/sec). This lesser velocity was considered sufficiently high to provide an indication of the cross-jet effect. A range of uniform tip clearances from 0.030 to 0.250 inch was obtained by raising or lowering the rotor segment with four jackscrews, and the clearances were set with a feeler gage.

The results of this investigation are shown in figure 9 for a constant supply pressure at the blade base. The coolant-air weight flow per blade and the ratio of tip static pressure to ambient static pressure are plotted against the rotor-tip clearance. At the maximum tip clearance of 0.250 inch, the static pressure indicated by the average of the six coolant-passage pressure taps located 1/32 inch inside the tip is essentially ambient pressure. As the tip clearance is reduced, the pressure ratio slowly increases to approximately 1.8 at 0.030-inch clearance. Thus the choking condition is apparently transferred from the coolant passage to the clearance space at low values of tip clearance. The coolant weight flow appears to be essentially unaffected by a reduction from 0.250 to 0.030-inch clearance, but further reduction in clearance would limit the weight flow because the clearance space is evidently choked as indicated by the pressure ratio. The effect of the cross flow from the other jet was negligible with respect to both weight flow and pressure throughout the system for the range of clearance investigated; but it is entirely possible that the arrangement of the jet does not adequately simulate full-scale conditions. Although the regular tolerance for tip clearances (0.060 to 0.090 in.) for standard blades provided adequate clearance for the flow of the coolant, an additional 0.015 inch was added to the cold-clearance dimension of the experimental blades to allow for possible high creep relative to the standard blades.

Turbine-Blade-Design Studies

Flow characteristics. - In order to facilitate fabrication,
the experimental blades were not twisted. At sections other than
at the hub, a different relative entrance angle and velocity dis-
tribution resulted for the experimental blade than with the stand-
ard twisted blades. When untwisted blades are used with standard
blades, the flow channels at either end of the cascade are consider-
ably modified near the blade tip (fig. 2); one passage converges
sharply, whereas the opposite channel diverges, probably with flow
separation and other undesirable conditions. Consequently, two
modified uncooled blades were used on this side of the test blade,
and one modified uncooled blade was used on the side adjacent to
the convergent channel.

When the relative entrance angles were investigated at sea-
level static conditions at 9000 rpm, the angle of attack at the
tip section was found to be much less than at the root, and the
relative angle was much less than for the standard blades. From
compressible-flow calculations, it did not appear that the velocity
distribution about the test blade was greatly affected by the end
conditions of the cascade although the lift produced by the blades
was reduced. Separation on the aft portion of the convex surface
of blades in static cascades is likely to occur even under ideal
entrance conditions; separated flow on the convex surface is there-
fore probable in these investigations.

The effect of the cooling air emerging at the tip on the
velocity distribution about the profile is unknown. The coolant
flow may fill the clearance space, in which case tip leakage and
other three-dimensional-flow aspects are considerably altered.

Blade stress limitations. - Stress analyses of the air-cooled
blade and the solid blade were made to estimate the permissible
speeds and metal temperatures. At 10,500 rpm, the computed simple
centrifugal stress at the root of the solid blade was 41,600 pounds
per square inch, which corresponds to an allowable temperature of
about 1250° F based on 1000-hour-life stress-rupture properties of
alloy X-40. Because of the uncertain stresses and the welded con-
struction at the blade base, the measured temperature of the solid
blade (thermocouples F and L) was limited to 1100° F or less dur-
ing operation. The blade-root stress in the hollow shell of the
cooled blade at 10,500 rpm was computed to be 32,200 pounds per
square inch, but the added weight of the tubes increased the stress
to 44,300 pounds per square inch, which corresponds to an allowable

temperature of 1220° F. Installation of thermocouples required deep cuts in the blade walls, which were later filled with braze metal that restored a part of the strength of the blades.

The welds used to attach the blade shells to the blade bases were checked by a tensile test at room temperature and found adequate. The method used for attaching the thermocouples and leads to the blades and the rotor was checked on a standard turbine in the engine up to rated speed (11,500 rpm).

EXPERIMENTAL PROCEDURE

General operating procedure. - Several series of runs at varied operating conditions were made during this investigation. For each series, the engine speed was maintained constant and the cooling-air weight flow through the blades was varied by manually operated valves located in the supply line. The adjustable exhaust nozzle was maintained at the fully open position for all runs. Because of the limited capacity of the slip-ring assembly, only six of the twelve rotating thermocouples could be connected for any one series.

Cooling investigations conducted. - The first investigation was devoted to the comparison of the temperatures of the cooled and the uncooled blades in one cascade with those at corresponding locations in the other cascade. Cooling-air temperatures at the inlet to the blade roots were similarly compared. The grouping of the thermocouples for this series was C-I, E-K, and F-L (fig. 5). Temperature readings obtained on the potentiometer from these thermocouples were compared to determine the uniformity of flow conditions. These runs were made at an engine speed of 4000 rpm. Investigations were then conducted first with the thermocouple grouping A, B, C, D, E, and F and then with the grouping G, H, I, J, K, and L at speeds of 4000, 6000, 8000, 9000, 10,000 and 10,500 rpm to determine the effect of the variation of the cooling-air flow on blade and cooling-air temperatures.

Before each series above 6000 rpm, a few points with different cooling-air flows were taken at either 4000 or 6000 rpm to check with previously obtained data. In this manner, malfunctioning of any part was detected. A visual check of any cracks or defects in the blades was made after speeds of 8000, 9000, and 10,000 rpm. No visible defects were noted.

Operating conditions. - The summary of conditions under which the investigations were conducted is given in table I for each series of runs made. For the various series, the engine speed varied from 4000 to 10,500 rpm, the engine combustion-gas flow varied from 18.8 to 61.5 pounds per second, and the turbine-inlet total temperature varied from 923° to 1293° F. The cooling-air flow per blade varied from 0.004 to 0.175 pound per second, and the temperature of the cooling air entering the root of the blade varied from 50° to 191° F.

CALCULATION PROCEDURES

Correlation of cooled-blade temperatures. - An approximate equation for determining the spanwise temperature distribution of the blade shell is given in reference 3. This equation, in the notation of the present report, is

$$\varphi = \frac{T_{g,e} - T_B}{T_{g,e} - T_{a,e,h}} = \frac{1}{1+\lambda} e^{-\frac{1}{1+\lambda}\frac{H_o l_o b}{c_{p,a} w_a}\frac{x}{b}} - \frac{\omega^2 w_a b}{gJH_o l_o(T_{g,e} - T_{a,e,h})}\frac{x}{b} +$$

$$\left(1 - e^{-\frac{1}{1+\lambda}\frac{H_o l_o b}{c_{p,a} w_a}\frac{x}{b}}\right)\left[\frac{\omega^2 w_a}{gJH_o l_o(T_{g,e} - T_{a,e,h})}\right]\left[\frac{c_{p,a} w_a (1+\lambda)}{H_o l_o} - r_h\right]$$

(1)

(Symbols are defined in the appendix.) In general, the second and third terms of this expression are negligible in comparison with the first term; also the quantity

$$e^{-\frac{1}{1+\lambda}\frac{H_o l_o x}{c_{p,a} w_a}}$$

in the first term does not vary appreciably. As a consequence

$$\varphi \approx \frac{\text{constant}}{1+\lambda}$$

(2)

where

$$\lambda = \frac{H_o l_o}{H_f l_i} \qquad (3)$$

where

H_o average gas-to-blade heat-transfer coefficient,
$(Btu/(sq\ ft)(^{\circ}F)(sec))$

H_f average blade wall-to-coolant heat-transfer coefficient,
$(Btu/(sq\ ft)(^{\circ}F)(sec))$

If the small effects of changes in the gas and cooling-air prop-
erties on the coefficients are neglected, it can be shown that

$$\lambda \approx constant\ \frac{w_g^m}{w_a^n} \qquad (4)$$

In some cases, the exponent m may be equal to n. On the basis
of equations (2) and (4), φ becomes a function of the coolant and
the gas flows,

$$\varphi \approx f(w_a, w_g) \qquad (5)$$

Thus as a first approximation, the temperature difference ratio φ
at each engine speed and for each thermocouple position on the
cooled blade can be plotted against the cooling-air flow. Such
curves are presented herein and should be approximately applicable
to all cooling-air and gas-temperature conditions.

    Correlation of solid-blade temperatures. - The effective gas
temperature $T_{g,e}$ is a term that must be known to determine φ ;
or if φ is known, to determine the blade temperature T_B. The
effective gas temperature is the temperature that an uncooled solid
blade, having the same profile as the cooled blade, would attain
under the same heating conditions as the cooled blade. In this
investigation, the temperature of the solid blade adjacent to the
cooled blade was used to determine the experimental values of φ.
In order to calculate the values of φ for a thermocouple posi-
tion, the temperature of the solid uncooled blade at a correspond-
ing thermocouple position should be used to be strictly correct.
Because of the limited number of thermocouples, the only tempera-
tures measured on the solid blades were on the leading edges (F and L).

These temperatures were used for the effective gas tempera-
ture $T_{g,e}$ in determining φ for all cooled-blade thermocouple
positions. Because the temperatures around uncooled solid blades
do not vary appreciably, only minor errors in the values of φ
will result.

In order to determine cooled-blade temperatures for any
engine condition and ultimately to determine whether these tem-
peratures exceed an allowable temperature, it is necessary to
derive a method of calculating the effective gas (solid-blade)
temperature based on gas-stream temperatures. The effective gas
temperature is related to the total and the static gas tempera-
tures through a recovery factor Λ, where

$$\Lambda = \frac{T_{g,e} - T_g}{T'_g - T_g} \tag{6}$$

The recovery factor Λ is also a function of Mach and Prandtl num-
bers of the gas. For low Mach numbers it has been shown (refer-
ence 10) that $\Lambda/\sqrt{Pr_g}$ is a function of the Mach number of the
gas.

In order to determine the recovery factor of the blades,
experiments were made using a static cascade of Lucite blades of
approximately the same profile as the modified rotor blades used
herein. The cascade of Lucite blades represented the rotor blades
of the turbine; however, no blades were placed upstream to repre-
sent nozzle blades. The resulting curve of $\Lambda/\sqrt{Pr_g}$ against the
Mach numbers of the gas at the inlet of the cascade is shown in
figure 10. This curve was used for calculating the solid-blade
leading-edge temperatures as follows:

Because no measurements were taken in the axial-clearance
space between the stator outlet and the rotor inlet, it was assumed
that the change in the gas properties was small in this space.
Consequently, the conditions at the rotor inlet are equal to those
at the stator outlet in the equations presented in this section.
At choking conditions of the nozzle, the expansion in this clear-
ance space was thus considered small with the result that the abso-
lute Mach numbers at both the stator outlet and the rotor inlet
were assumed equal to 1. If agreement is attained between the cal-
culated and the measured values of the solid-blade temperatures,
the assumption made can be considered sufficiently valid for the
engine investigated.

The Mach number at the rotor inlet was calculated from the equation

$$M_{g,R,I} = \frac{W_{g,R,I}}{\sqrt{\gamma_g g R_g \, T_{g,S,E}}} \tag{7}$$

where

$W_{g,R,I}$ relative velocity of gas at rotor inlet, (ft/sec)

$T_{g,S,E}$ static temperature of gas at stator outlet, ($^{\circ}$R)

The relative velocity was calculated by assuming α to be a constant from the stator exit to the rotor inlet and by using the expression

$$W_{g,R,I} = \sqrt{V_{g,S,E}^2 + U^2 - 2V_{g,S,E} \, U \cos \alpha} \tag{8}$$

where

$V_{g,S,E}$ velocity of gas at stator outlet, (ft/sec)

U velocity of rotor at midspan of blades, (ft/sec)

α stator-blade exit angle at midspan of blades (relative to plane normal to engine axis), (deg)

With the assumptions that the total pressure and temperature at the stator outlet are equal to the values at the stator inlet, it can be shown that at the throat of the nozzle

$$\left[\left(\frac{p_{g,S,E}}{p'_{g,S,I}}\right)^{\frac{2}{\gamma_g}} - \left(\frac{p_{g,S,E}}{p'_{g,S,I}}\right)^{\frac{\gamma_g+1}{\gamma_g}} \right] = \left(\frac{w_g}{A_{S,E} p'_{g,S,I}}\right)^2 \frac{\gamma_g - 1}{2\gamma_g g} R_g T'_{g,S,I} \tag{9}$$

All values on the right side of equation (9) were calculated directly from the data. Thus, the stator-outlet static-to-total pressure ratio could be calculated. With the ratio and $p'_{g,S,I}$ known, the static pressure was obtained. Then the stator-outlet static temperature was calculated from

$$T_{g,S,E} = T'_{g,S,I} \left(\frac{p_{g,S,E}}{p'_{g,S,I}} \right)^{\frac{\gamma_g - 1}{\gamma_g}} \tag{10}$$

The velocity $V_{g,S,E}$ needed in equation (8) was calculated from the continuity equation

$$w_g = V_{g,S,E} \, A_{S,E} \frac{p_{g,S,E}}{R_g T_{g,S,E}} \tag{11}$$

After determining $M_{g,R,I}$, the factor $\Lambda/\sqrt{Pr_g}$ was obtained using figure 10. The value Pr_g was evaluated, at the temperature $T_{g,S,E}$, as calculated from equation (10). The effective gas temperature was then calculated using the value of Λ so determined and the equation

$$\Lambda = \frac{T_{g,e} - T_{g,S,E}}{T''_{g,R,I} - T_{g,S,E}} = \frac{T_{g,e} - T_{g,S,E}}{(W_{g,R,I})^2/2Jgc_{p,g}} \tag{12}$$

Plots of calculated $T_{g,e}$ against the measured solid-blade temperatures were made in order to determine the efficacy of this method for calculating $T_{g,e}$ for the engine conditions U, $p'_{g,S,I}$, $T'_{g,S,I}$, and w_g. The values of these four engine conditions are the parameters needed to calculate the effective gas temperature. For the case of sonic velocity at the nozzle exit, equation (9) can be eliminated, equation (10) can be replaced by

$$T_{g,S,E} = \frac{2}{\gamma_g + 1} T'_{g,S,I} \tag{13}$$

and equation (11) can be replaced by

$$V_{g,S,E} = \sqrt{\gamma_g g R_g \frac{2}{\gamma_g + 1} T'_{g,S,I}} \tag{14}$$

The data indicated that for the engine investigated, sonic velocity at the nozzle exit occurred at speeds of about 8000 rpm and above.

The specific-heat ratio γ_g, the specific heat $c_{p,g}$, and the gas constant R_g needed to solve equations (7) to (14) were evaluated at the static temperature at the turbine-nozzle outlet $T_{g,S,E}$ and at the fuel-air ratio of the combustion gases and the hydrogen-carbon ratio of the fuel used.

Calculation of total temperature of mixture in tail pipe. - When the total and static pressures measured in the tail pipe and the indicated temperature at this location are used, the static temperature of the mixture in the tail pipe T_m can be obtained by

$$T_m = \frac{(T_m)_{ind}}{1 + 0.6\left[\left(\dfrac{p'_m}{p_m}\right)^{\frac{(\gamma_m - 1)}{\gamma_m}} - 1\right]} \qquad (15)$$

The factor 0.6 represents the recovery factor for the tail-pipe thermocouples. The values of γ_m were based on the true mixture temperature and the fuel-air ratio of the mixture, and the hydrogen-carbon ratio of the fuel.

The total temperature T'_m was obtained from the relation

$$T'_m = T_m \left(\frac{p'_m}{p_m}\right)^{\frac{\gamma_m - 1}{\gamma_m}} \qquad (16)$$

Caclulation of turbine-inlet temperatures. - As stated in the previous section, the turbine-inlet total temperatures were required in calculating the solid-blade or effective gas temperature. Because of the variation of gas temperature at the turbine inlet, it was difficult to obtain a good average value of this temperature without use of a large number of thermocouples. As a consequence, the turbine-inlet total temperature $T_{g,S,I}$ was calculated.

With the assumption that the heat released by the main gas stream in the tail pipe is equal to that gained by the coolant, the scavenge, and the bearing-cooling air inside the tail

cone, the energy equation for the flow through the turbine and the tail pipe is as follows (See reference 11 for details.):

$$(w_g h'_{g,S,I} - P_c - Q_{a,B}) + (w_a h'_{a,I} + P_a + Q_{a,B} + Q_{a,t}) +$$

$$(w_s h'_{s,I} + Q_{s,t}) - Q_{a,t} - Q_{s,t} = w_m h'_m \qquad (17)$$

where

$h'_{a,I}$ total enthalpy of blade-cooling air before entering tail cone, (Btu/lb)

$h'_{g,S,I}$ total enthalpy of combustion gases at stator inlet, (Btu/lb)

h'_m total enthalpy of mixture of combustion gases, blade-cooling air, scavenge air, and bearing-cooling air in tail pipe, (Btu/lb)

$h'_{s,I}$ total enthalpy of scavenge and bearing-cooling air before entering tail cone, (Btu/lb)

P_a power to pump blade cooling air, (Btu/sec)

P_c power required by compressor, (Btu/sec)

$Q_{a,B}$ heat gained by cooling air passing through cooled blades, (Btu/sec)

$Q_{a,t}$ heat gained by blade-cooling air from tail pipe, (Btu/sec)

$Q_{s,t}$ heat gained by scavenge and bearing-cooling air from tail pipe, (Btu/sec)

w_g weight-flow rate of combustion gas, (lb/sec)

w_m weight-flow rate of mixture of fluids in tail pipe, (lb/sec)

w_s weight-flow rate of scavenge and bearing-cooling air, (lb/sec)

Because P_a is very small it can be neglected and equation (17) can be solved for $h'_{g,S,I}$ as follows:

$$h'_{g,S,I} = \frac{w_m h'_m - (w_a h'_{a,I} + w_s h'_{s,I}) + P_c}{w_g} \qquad (18)$$

The power required by the compressor equals

$$P_c = (h'_{A,c,E} - h'_{A,c,I})\frac{w_g}{1 + f} \qquad (19)$$

thus

$$h'_{g,S,I} = \frac{w_m}{w_g} h'_m - \frac{w_a}{w_g} h'_{a,I} - \frac{w_s}{w_g} h'_{s,I} + \frac{(h'_{A,c,E} - h'_{A,c,I})}{1 + f}$$

$$(20)$$

The enthalpy values of the combustion air at the compressor inlet and outlet were based on measured total temperatures. The values of fuel-air ratio f were also obtained from data. The total enthalpies of the blade-cooling, scavenge, and bearing-cooling air before the air entered the tail cone were based on temperatures measured just downstream of the flow measuring orifices. The enthalpy of the gaseous mixture h'_m was based on the fuel-air ratio existing in the tail pipe and on the total temperature in the tail pipe T'_m. These enthalpies were obtained from charts given in reference 12.

After solving equation (20) for the enthalpy of the combustion gases at the turbine inlet, the total temperature at this station was determined again using the charts of reference 12. The fuel-air ratio of the combustion gases was used in this determination.

Calculation of turbine-inlet pressures. - The turbine-inlet total pressures, also needed in the determination of the solid-blade temperatures (equation (9)), were obtained by using the measured compressor-outlet pressures and subtracting a 5-percent pressure loss through the combustion chambers. Use of the value 5 percent is valid for this type of engine on the basis of results and assumptions presented in reference 13.

Cooling-air temperatures. - In the present investigation, the cooling-air temperature was measured in the radial cooling-air-inlet passage slightly below the blade base. For the purpose of simplification of the instrumentation, no rotating pressure measurements were obtained in the cooling-air passages, and as a

consequence it was impossible to determine an effective cooling-
air temperature from the measured temperature by methods similar
to those used to obtain the effective gas temperature. The meas-
ured temperature in the radial passages was therefore used for
$T_{a,e,h}$ in the calculation of φ values. Because of the small
amount of heat that was picked up by the air from this position in
the tube to the blade root and because the recovery factors for
the thermocouples were roughly of the same magnitude as for the
tube passages, the use of this measured temperature in the tube
for $T_{a,e,h}$ should lead to little error in the temperature ratio
when this ratio is compared with a theoretically obtainable value.

Properties of combustion gases and cooling air. - In the cal-
culations, the Prandtl number, the specific heats, and the ratio
of specific heats for both the cooling air and the combustion gases
were obtained from the data in references 14 and 15. The hydrogen-
carbon ratio of the fuel used was 0.155.

RESULTS AND DISCUSSION

The results of the experimental investigation of air-cooled blades
consisting of a blade shell with ten tube inserts are presented
in figures 11 to 18 and are discussed in the following paragraphs.

Experimental Data

Comparison of blade and cooling-air temperatures. - The
results of the first series of runs, which were made to compare
the temperatures of the cooled and uncooled blades at approximately
the same locations and to compare the temperatures of the cooling
air at the root of each air-cooled blade, are shown in figure 11.
The cooling-air temperature at the root of one blade (thermo-
couple E) is compared in figure 11(a) with that at the root of the
other blade (thermocouple K). The agreement between the two read-
ings was good as evidenced by the 45° line, which represents a
mean of the data points. The same agreement existed for the two
readings of leading-edge temperatures of the two solid blades
(thermocouples F and L). The data points fall along a 45° line
with no deviation, as shown in figure 11(b). The agreement
between measurements of temperatures at the trailing edges of the
two air-cooled blades, also shown in figure 11(b), was not so good
as that for the solid blades, but the data did fall around a
45° line.

From these data, it was concluded that similar conditions of
gas flow, cooling-air flow, and so forth were obtained through the
two diametrically opposite modified cascades and that temperatures
measured on one rotating cascade could be combined with tempera-
tures on the other, for the same conditions, for purposes of
obtaining an over-all study of blade temperatures.

Effect of engine speed and cooling-air flow on blade, effec-
tive gas, and cooling-air temperatures. - The experimental data
taken during the investigation for three engine speeds are pre-
sented in figure 12. Solid-blade temperatures or effective gas
temperatures, cooled-blade temperatures, and cooling-air tempera-
tures are plotted against cooling-air-flow rate per blade for each
speed. Figures 12(a) and 12(b) are for a low speed, 4000 rpm;
figures 12(c) and 12(d) are for a medium speed, 8000 rpm; and fig-
ures 12(e) and 12(f) are for a high speed, 10,000 rpm. The engine
temperature conditions corresponding to the results in figure 12
are presented in table I. Although cooling air passed through the
blades at rates as high as 0.175 pound per second per blade, only
data up to approximately 0.10 pound per second per blade are shown
because little cooling effect was obtained for higher flow rates.

Appreciable cooling of the air-cooled blades resulted even at
low cooling-air flows. The midchord temperatures of the blades
were very low, in some cases being less than one-half that of the
solid blades. For example, at 10,000 rpm (fig. 12(f)), the
modified-uncooled-blade temperature was about 960° F, and the mid-
chord temperatures averaged about 470° F at a cooling-air flow of
0.07 pound per second per blade. The leading- and trailing-edge
temperatures for the same coolant-flow rate were much higher; as
much as 300° and 350° F, respectively, above the midchord tempera-
tures although still 160° F lower than the solid-blade temperatures.
Good over-all cooling requires a reduction of these leading and
trailing-edge temperatures to values which approach that of the
midchord.

As the cooling-air flow was decreased at low speeds, the tem-
perature of the blade at the trailing edge near the tip (thermo-
couple A) at first increased, as expected, then because of some
unknown characteristic of the coolant flow the temperature
decreased (fig. 12(a)). With further decrease in coolant flow,
the temperature began to rise again. This dip in the curve per-
sisted throughout the speed range. Some clue to the cause of this
phenomenon may be in the general behavior pattern observed. As
the speed increased, this noncharacteristic behavior became evident
at progressively higher values of coolant-flow rate.

The slight drop in the temperature of the leading-edge of the
modified-uncooled blade is attributed to the drop in the compressor-
inlet temperature as the ambient temperature of the test cell
decreased.

Correlated Cooled-Blade Temperatures

According to equation (5), the temperature ratio φ or
$(T_{g,e} - T_B)/(T_{g,e} - T_{a,e,h})$, is approximately a function of the
cooling-air and combustion-gas weight flows. Curves that show the
variation of the temperature ratio φ with cooling-air flow are
therefore presented in figure 13. Each part of figure 13 repre-
sents results for a particular thermocouple location and includes
curves for several engine speeds and, consequently, gas flows.

Except for the trailing-edge temperatures at the blade tip
(fig. 13(a)), the data for each thermocouple location could be
represented by a set of curves (figs. 13(b) to (g)). For a given
coolant-flow rate as engine speed increased, the values of φ
generally decreased, which corresponds to an increase in blade
temperature. In some instances, for example, trailing-edge ther-
mocouples C and D (figs. 13(c) and (d)), straight lines having a
common slope represented the data reasonably well for all speeds
over the upper portion of the coolant-flow range. It was neces-
sary, however, to alter the slope of the lines in order to extend
the representation to the lower portion of the coolant-flow range.
The drooping of the curves for thermocouples H and J at low
coolant-flow rates and high engine speeds was verified by means
of equation (1) using heat-transfer coefficients for a ten-tube
blade based on static-cascade investigations. In a subsequent
section of this report, these curves are used to predict blade
temperatures for various conditions of gas and cooling-air tem-
peratures, cooling-air flow, and so forth. The only known errors
associated with the method are those due to discrepancies in
extrapolation technique and neglect of changes in the properties
of the gas and the air, as pointed out in the calculation
procedures.

The data of figure 13(c) are plotted in another manner in
figure 14. Equation (5) shows that φ is a function of coolant-
and gas-flow rates. Experimental values of φ were divided by
the corresponding measured cooling-air-flow rates raised to a
power n. The values of n represent the slopes of the curves
in figure 13(c). The resulting values of $\varphi/w_a{}^n$ were plotted

against the gas-flow rate for each speed. Because two values of the slope are required to represent closely the data in figure 13(c), two curves result; one for the low cooling-air-flow rates, n = 0.10, and one for the high flow rates, n = 0.223. Although some data points may appear to be quite far from the curves, the most extreme deviation of a data point from an average line would have a very small effect on the calculated blade temperature.

Data that follow a trend as shown by thermocouple C (fig. 13(c)) are the only ones that can be represented by generalized curves, as shown in figure 14. In calculating allowable turbine-inlet temperatures for various coolant flows and other conditions, it is usually the trailing-edge-temperature curves that are used for predictions. These curves are used because the highest temperatures usually occur at the trailing edge.

The variations of blade temperature with both gas flow (or speed) and cooling-air flow for all thermocouples followed regular patterns with the exception of thermocouples A, H, and J (fig. 13). The variation of temperatures at H and J with speed for a fixed ratio of cooling-air flow to gas flow were irregular above speeds of about 7000 rpm. The variation of the cooled-blade temperature at the midchord (thermocouple J) with engine speed is presented in figure 15. For two coolant-flow rates the blade temperature T_B was calculated for a constant effective gas temperature $T_{g,e}$ of 1000° F and a coolant temperature $T_{a,e,h}$ of 80° F. The variation in the blade temperature as shown in figure 15 may be caused by free convection canceling the forced-convection cooling. At an engine speed of 8750 rpm, the velocity profile in the boundary layer is probably perpendicular to the wall. Such a situation would reduce the inside film coefficient to a minimum, thus accounting for the peaks in the temperature curve. Above 8750 rpm, cooling is taking place through a free-convection-flow system that is hampered by the forced flow through the center of the tube. Conversely, below 8750 rpm, cooling is occurring through a forced-convection system and is retarded by free convection. Further research is necessary to verify this reasoning. Thermocouple H temperatures also showed fluctuation above about 7000 rpm but not to the extent evidenced by thermocouple J.

Correlated Solid-Blade Temperatures

A comparison of the calculated and measured solid-blade temperatures for the several turbine speeds investigated is shown in figure 16. A 45° line on the plot is a well represented mean of

the data points. Calculated cooled-blade temperatures based on
the φ curves of figure 13 would be only slightly affected by the
most extreme deviation of a data point from the line in figure 16.
It is therefore concluded that effective gas or solid-blade tem-
peratures can be calculated by the procedures given with satisfac-
tory accuracy for the range of temperatures measured (850° to
1100° F); and the assumption that the change in the gas properties
is small in the axial-clearance space between the stator outlet
and the rotor inlet was sufficiently valid for the engine investi-
gated. This assumption may not be true for other engines where
the expansion in the clearance space may be appreciable. In such
a case, measurements at the rotor inlet must be obtained to cal-
culate the solid-blade temperature.

Cooling-Air-Temperature Increase Through Radial Passages

Although the method of introducing air into the two cooled-
blade roots by use of radial passages shown in figure 3 was pecul-
iar to this setup and is probably greatly different from methods
that will be used when all the blades are cooled, the rise in
cooling-air temperature through the passages $(t_{a,e,h} - t_{a,H})$
would probably be of interest in determining the order of magni-
tude of the increase. Cooling-air-temperature rises from as low
as 8° F to as high as 100° F were obtained depending on the con-
ditions. Complete data for this part of the investigation are
shown in figure 17. The increase in temperature from the hub to
the blade root is plotted against cooling-air flow per blade for
the several engine speeds. On the log-log plot presented, a
straight line was considered as representative of the data for
each speed.

Blade Failure

The investigation of the first blade configuration was ter-
minated by failure of one of the cooled blades at an engine speed
of 10,500 rpm. The failure occurred as the run at this speed was
nearing completion, at which time the rate of cooling-air flow to
the blade was small. The blade that failed was the one that was
instrumented to obtain temperatures at positions G, H, I, and J
(fig. 4). From the inspection of the portion of the broken blade
remaining in the rotor (fig. 18), failure appeared to have occurred
along the groove that was cut for thermocouple J and at the root
of the blade where three thermocouple leads came out of the base
of the blade. These failure points are noted in figure 18.

PREDICTIONS OF ALLOWABLE TURBINE-INLET TEMPERATURE

General Method

Although the blade temperatures obtained from given engine
conditions are of great interest, of more interest is the allow-
able turbine-inlet temperature for a given blade configuration,
method of blade construction, and material. Consequently, on the
basis of cooling results presented herein calculations were made
of allowable turbine-inlet temperatures for the present configura-
tion at design speed of the engine, 11,500 rpm. The general method
of determining these allowable temperatures is to establish first
the allowable-blade-temperature distribution from root to tip for
the design speed. For the blade concerned, only the simple radial-
centrifugal-stress distributions were calculated. From this cal-
culated stress distribution and the curve of stress-to-rupture
against metal temperature based on 1000-hour life for the material
considered, an allowable radial temperature distribution was deter-
mined. For the engine at rated speed, an example of a resulting
allowable blade-temperature-distribution curve for high-temperature
alloy X-40 is shown by the dashed line in figure 19 for two
methods of blade fabrication described in the figure.

The allowable turbine-inlet temperature for a given engine
condition was calculated from the allowable effective gas tempera-
ture. The allowable effective gas temperature, for a given cool-
ant temperature at the blade root, coolant-flow rate, and gas-flow
rate, was obtained from the extrapolated values of temperature ratio φ
for the trailing-edge thermocouples by assuming values of the effec-
tive gas temperature $T_{g,e}$ and then calculating the blade-radial-
temperature distribution and plotting curves of this distribution.
The assumed value $T_{g,e}$, which causes such a curve to be tangent to
the allowable blade-metal-temperature curve is the allowable value
sought for the case where the tubes are supported by the blade
base (fig. 19(b)). For the blade with the shell supporting the
tubes, the allowable blade-metal-temperature is found at the point
of intersection of the two curves, which is at the blade base
where the lowest allowable blade temperature exists (fig. 19(a)).
This permissible blade temperature is a minimum at the base
because the centrifugal stresses of both shell and tubes are dis-
tributed over the cross-sectional area of the shell alone at this
position. At an incremental distance above this position the
stresses are distributed in both tubes and shell, which accounts
for the sudden discontinuity in the curve in figure 19(a). For

the case of the blade with base supporting both shell and tubes, tangency of the allowable and calculated blade-temperature-distribution curves occurs at a point away from the base, as shown in figure 19(b).

The gas flow and compressor-outlet temperatures at a given engine speed and engine-inlet condition were determined from the curves in figure 20, which were obtained from the experimental data. Although in the experimental investigation the cooling air was supplied by an independent source, in the present calculations it was assumed that the cooling air was bled off at the compressor outlet. The curve of figure 20(a) was used to determine the compressor-outlet temperature at a given speed and inlet condition. The gas-flow rate was obtained from figure 20(b), although this value of w_g was slightly high for the assumption of the cooling air bled from the compressor. The error incurred by using figure 20(b) to obtain w_g was small because of the small effect of gas flow on the value of φ for the conditions used and because small cooling-air-flow rates were assumed. Standard sea-level conditions were used for $T'_{a,c,I}$ and $p'_{a,c,I}$.

A ratio of blade-coolant to combustion-gas-flow rate of 0.05 was assumed; then if w_g is known, w_a can be calculated. The temperature of the coolant at the blade root was equal to the temperature at the hub, which was assumed equal to the temperature of the air at the compressor outlet, plus the temperature rise through the rotor passages obtained from figure 17. This value of coolant temperature at the blade root is probably higher than would be encountered in an engine that was primarily designed for turbine cooling because in the engine investigated the method of passing the air through the rotor is very inefficient. In another case, it was assumed that a heat exchanger was inserted between the compressor and the turbine for cooling the blade-cooling air and $T_{a,e,h}$ was assumed.

With $T_{g,e}$ and w_g known, the calculation of allowable turbine-inlet temperature $T'_{g,S,I}$ was also a trial-and-error solution. At design speed the nozzle-exit velocity was sonic. An assumption of $T'_{g,S,I}$ was made and $T_{g,S,E}$ and $V_{g,S,E}$ were calculated using equations (13) and (14). The relative velocity was then calculated using equation (8) and then the relative Mach number using equation (7). The recovery factor Λ was obtained using the relative Mach number and figure 10. The factors obtained and equation (12) were then used to calculate $T_{g,e}$. This calculated value of $T_{g,e}$ was compared with the value of allowable $T_{g,e}$

that produced the tangency or intersection of the allowable temperature and the calculated blade-temperature-distribution curves. If the two values did not agree, new values of $T'_{g,S,I}$ were assumed until agreement was obtained. The value of $T'_{g,S,I}$ for which agreement between these values of $T_{g,e}$ was obtained constitutes the allowable turbine-inlet temperature sought for the condition of the calculation.

The allowable turbine-inlet temperatures were also calculated for the case of a fictitious-blade configuration having a uniform chordwise temperature distribution equal to that of thermocouple J. In other words, it was of interest to know the calculated allowable turbine-inlet temperature for a blade uniformly cooled chordwise at the temperature that existed at the midchord of the configuration investigated. These computations indicate the potential value of further blade investigations.

The calculations were similar to those just described with the exception that along the midchord no spanwise temperature-distribution data had been obtained. As a consequence, only one point on a curve such as the solid curve in figure 19 could be calculated. The remainder of the curve was sketched in with a shape similar to the trailing-edge spanwise-distribution curves.

Conditions for Allowable Temperature Calculations

The calculations were performed considering blades made of either of two materials, one a high-temperature alloy X-40, and one having a low critical-alloy content, Timken alloy 17-22A. The Timken alloy has a low strategic metal content (Cr, 1.29 percent; Mo, 0.52 percent; V, 0.25 percent) and consequently satisfies the first objective of the study, namely, effective use of less-strategic materials.

Further conditions of the calculations set the cooling-air temperatures at the blade root at 506° and 200° F. The temperature of 506° F is the calculated value obtained when air is bled directly from the compressor and the temperature of 200° F is the assumed temperature previously mentioned for the case of an intercooler placed between the compressor and the turbine in the blade cooling-air line.

1410

The calculations were made on the basis that the trailing-edge temperatures comprise the limiting condition and also on the basis that the whole blade was as effectively cooled as the midchord of the blade reported herein.

Finally, the method of blade fabrication was considered as part of the conditions. In one method, the blade was assumed to be made in the same manner as the blades used in the present investigation; that is, the blade shell supporting the tubes and the shell attached to the base. In the other method, the blade was presumably designed so that the tubes and the shell were both supported at the base by extending the tubes and brazing them into the base. The stress calculations for both designs were made for blades with the slight taper of the modified blades used in the present investigation. Actual production blades would probably have a greater taper and, as a consequence, the allowable-temperature curves (fig. 19) are lower than if tapered blades had been considered.

Allowable Temperatures for Nonstrategic Metals

Blades with tubes supported by shell. - The summary of the results of allowable turbine-inlet temperatures for the conditions used is shown in table II. For the nonstrategic metal, Timken alloy 17-22A, the tubes supported by the shell, the air bled direct from the compressor, and on the basis of trailing-edge temperatures, calculations indicated a permissible turbine-inlet temperature of 1370° F. If an air temperature of 200° F was used, which was obtained by some means such as the use of an intercooler, the other conditions remaining constant, the results indicated that a temperature of 1450° F was permissible.

Calculations based on a fictitious configuration having a uniform chordwise temperature distribution equal to the observed temperature at the midchord of the experimental blade configuration show the permissible turbine-inlet temperatures without and with an intercooler to be 2090° and 2585° F, respectively. The other conditions are the same as in the preceding paragraph.

Blades with tubes supported by base. - When the blade shell and the tubes were supported by the base, the calculations indicated that the allowable turbine-inlet temperatures were the same as for the previous method of fabrication even though the stress at the base was higher for the other method of fabrication. The reason is that the allowable metal temperature for alloy 17-22A

changes little within the stress range considered with the conse-
quence that the stress at the base of the blade is not the limit-
ing condition. The point of tangency of the allowable temperature
and the calculated blade temperature occurs at a position above
the base.

The practicality of using air-cooled turbine blades made with
a nonstrategic material at present turbine-inlet gas temperatures
is evident from these calculations. Although the calculated
turbine-inlet temperatures based on the trailing-edge temperature
are below the present allowable turbine-inlet temperatures, these
temperatures can be increased. Blades having better stress dis-
tributions, that is, greater tapers and larger root areas, will
allow higher trailing-edge temperatures than those calculated.
Further investigation on methods of cooling of the trailing edges
should also yield improvements. The obvious advantage of increas-
ing the cooling effectiveness at the trailing and leading edges is
seen in table II by comparison of the calculated allowable turbine-
inlet temperatures based on the trailing edge with those based on
the midchord temperatures. Further increase in allowable turbine-
inlet temperature can be realized when an intercooler is intro-
duced in the system. The advantage of decreasing the cooling-air
inlet temperature becomes more pronounced as the turbine-inlet
temperature increases and as the temperature-difference ratio φ
increases; of course, the attendant advantages as well as the
incurred disadvantages need further study.

Allowable Temperatures for Strategic Metals

Blades with tubes supported by shell. - The calculated allow-
able turbine-inlet temperature for a blade of high-temperature
material, X-40, is 1615° F based on trailing-edge temperatures,
cooling-air bled direct from compressor, and the tubes supported
by the shell (table II). If an intercooler is installed between
the compressor and the turbine the allowable temperature is
increased to 1795° F.

For the same conditions except for an assumed uniform tempera-
ture distribution based on the observed values at the midchord,
the allowable temperatures without and with an intercooler are com-
puted to be 2600° and 3280° F, respectively.

Blades with tubes supported by base. - When it is assumed
that the blade tubes and the shell are supported by the base, the
calculations for blades of X-40 show that for air bled from the

compressor the allowable temperature, based on trailing-edge tem-
peratures, was 1770° F. Use of an intercooler increases the value
to 1870° F. On the midchord temperature basis, these temperatures
are increased to 2900° and 3420° F, respectively.

    The results of the calculations indicate that much higher
allowable turbine-inlet temperatures are possible but at the pre-
mium of using high-temperature alloys.

    These calculations are based on simple centrifugal-stress cal-
culations and do not include thermal or vibratory stresses; there-
fore the values listed in table II may be optimistic for the
blades investigated. However, the blades investigated had little
taper from root to tip. The radial stress distribution was there-
fore none too favorable with the result that the allowable
turbine-inlet temperatures were reduced. From these considera-
tions and the fact that the gas dissociation was not considered in
the calculations, the values in table II are thought nevertheless
to be representative of the possible turbine-inlet temperatures
with air-cooled blades.

<p style="text-align:center">SUMMARY OF RESULTS</p>

    The investigation was conducted to determine experimentally
the effectiveness of air cooling turbine blades in a production
turbojet engine, which was modified and instrumented for the pur-
pose. The results of this investigation of a blade shell with
10 tube inserts were as follows:

    1. The midchord of the blade cooled satisfactorily, whereas
the leading- and trailing-edge temperatures were unsatisfactorily
high for the configuration used. For example, at an engine speed
of 10,000 rpm, a cooling-air temperature of 100° F at the blade
root, and a cooling-air-flow rate per blade about 6 percent of the
gas-flow rate per blade, the trailing-edge, the leading-edge, and
the average of the midchord temperatures were about 790°, 760°,
and 470° F, respectively, as compared with about 960° F for the
modified-uncooled blade.

    2. The temperature data for most thermocouple positions were
correlated for the conditions investigated by plotting the ratio
of the difference between the solid-blade and cooled-blade tempera-
tures to the difference between the solid-blade and cooling-air at
blade-root temperatures against cooling-air-flow rate for each

engine speed. On the basis of theory, such a correlation was applicable with small error to predictions of blade temperatures for other conditions than those investigated.

3. A method of calculating solid-blade temperatures for any engine conditions using data on recovery factors obtained from cascade experiments showed that the measured temperatures could be predicted within an accuracy of 20° F for a range of indicated temperatures from about 850° to 1100° F.

4. Temperature increases of the cooling air from the rotor center line to the cooled-blade root from 8° to 100° F were measured depending on engine speed and cooling-air-flow rate.

5. On the basis of temperatures obtained on the blades used in this investigation, calculations showed that, with cooling, turbine-inlet temperatures of 1370° F at rated speed possibly could be obtained with the nonstrategic metal Timken alloy 17-22A. The calculations were based on trailing-edge temperatures as the limiting ones for a blade with tubes and shell supported by the base and on the assumption of standard sea-level compressor-inlet conditions, cooling-air bled off at the compressor outlet, and a ratio of cooling-air-flow rate to gas-flow rate of 5 percent.

6. Assuming a uniform chordwise temperature distribution with a temperature equal to that obtained at the midchord of the blade investigated, calculations indicated that the allowable turbine-inlet temperature could be increased from 1370° to 2090° F.

7. At high turbine-inlet temperatures, an intercooler located in the cooling-air system between the compressor and the turbine was shown by calculations to have an appreciable effect on the allowable turbine-inlet temperature. For example, an allowable turbine-inlet temperature of 2090° F was determined for cooling-air temperature at the blade root of 506° F as bled directly from the compressor. If through an intercooler the coolant-inlet temperature was reduced, the predicted turbine-inlet temperature was raised to 2585° F.

Lewis Flight Propulsion Laboratory,
    National Advisory Committee for Aeronautics,
        Cleveland, Ohio, July 30, 1950.

1410

EXPERIMENTAL INVESTIGATION OF AIR-COOLED

TURBINE BLADES IN TURBOJET ENGINE

I - ROTOR BLADES WITH 10 TUBES IN

COOLING-AIR PASSAGES

Herman H. Ellerbrock, Jr.,
Aeronautical Research
Scientist.

Francis S. Stepka,
Aeronautical Research
Scientist.

Approved: Herman H. Ellerbrock, Jr.,
Aeronautical Research
Scientist.

Oscar W. Schey,
Aeronautical Research
Scientist.

jg

APPENDIX - SYMBOLS

The following symbols are used in this report:

A   cross-sectional flow area (perpendicular to direction of
       flow), sq ft

b   blade height or span, ft

c_p specific heat of fluid at constant pressure, Btu/(lb)(°F)

f   fuel-air ratio

g   acceleration due to gravity, ft/sec^2

H_f average blade-wall-to-coolant heat-transfer coefficient,
       Btu/(sq ft)(°F)(sec)

H_o average gas-to-blade wall heat-transfer coefficient,
       Btu/(sq ft)(°F)(sec)

h'   total enthalpy, Btu/lb

J   mechanical equivalent of heat, 778 ft-lb/Btu

k   thermal conductivity of fluid, Btu/(°F)(ft)(sec)

l perimeter of cooled blade, ft

M   Mach number

m   exponent

N   engine speed, rpm

n   exponent

P   power, Btu/sec

p   static pressure, lb/sq ft

p'   total pressure, lb/sq ft or in. Hg

Pr   Prandtl number, $c_p \mu g/k$

Q   heat gained, Btu/sec

R   gas constant, ft-lb/(lb)(°F)

r   radius from center of rotor, ft

T   static temperature, °R or °F

T'   total temperature, °R or °F

T"   total temperature relative to moving rotor blades, °R

U   tangential or peripheral velocity at midspan of rotor blades, ft/sec

V   absolute velocity, ft/sec

W   relative velocity, ft/sec

w   weight flow rate, lb/sec

x   distance from blade root to blade element, ft

α stator-blade exit angle at midspan of blade, deg (relative to plane normal to engine axis)

γ ratio of specific heats

Λ temperature recovery factor of modified solid blade

λ $H_o l_o / H_f l_i$

μ absolute viscosity of fluid, slugs/(ft)(sec)

φ temperature-difference ratio, $(T_{g,e} - T_B)/(T_{g,e} - T_{a,e,h})$

ω angular velocity of rotor, radians/sec

Subscripts:

A   combustion air

a   blade-cooling air

B   cooled blade

c   compressor

E   exit or outlet

e   effective

F   fuel

g   combustion gas

H   hub of rotor

h   root of blade

I   inlet

i   inside

m   mixture of combustion gas and scavenge, bearing, and blade-
        cooling air in tail pipe

o   outside

R   rotor

S   stator

t   tail pipe

s   scavenge, and bearing-cooling air

ind   refers to measured value of temperature

REFERENCES

1. Hubbartt, James E.: Comparison of Outside-Surface Heat-Transfer
   Coefficients for Cascades of Turbine Blades. NACA RM E50C28,
   1950.

2. Freche, John C., and Diaguila, Anthony J.: Heat-Transfer and
   Operating Characteristics of Aluminum Forced-Convection and
   Stainless-Steel Natural-Convection Water-Cooled Single-Stage
   Turbines. NACA RM E50D03a, 1950.

3. Livingood, John N. B., and Brown, W. Byron: Analysis of Span-
   wise Temperature Distribution in Three Types of Air-Cooled
   Turbine Blades. NACA Rep.

4. Brown, W. Byron, and Rossbach, Richard J.: Numerical Solution of Equations for One-Dimensional Gas Flow in Rotating Coolant Passages. NACA RM E50E04, 1950.

5. Ellerbrock, Herman H., Jr., and Schafer, Louis J., Jr.: Application of Blade Cooling to Gas Turbines. NACA RM E50A04, 1950.

6. Schramm, Wilson B., Nachtigall, Alfred J., and Arne, Vernon L.: Preliminary Analysis of Effects of Air Cooling Turbine Blades on Turbojet-Engine Performance. NACA RM E50E22, 1950.

7. Livingood, John N. B., and Sams, Eldon W.: Cooling of Gas Turbines. VI - Computed Temperature Distribution through Cross Section of Water-Cooled Turbine Blade. NACA RM E7B11f, 1947.

8. Dempsey, W. W.: Turbine Blade Cooling (Final Hot Test Rep.). No. 2037, Stalker Development Co., June 29, 1949.

9. Kuepper, K. H.: Temperature Measurement on Two Stationary Bucket Profiles for Gas Turbines with Boundary-Layer Cooling. Trans. No. F-TS-1543-RE, Air Materiel Command, U.S. Air Force, Jan. 1948. (ATI No. 18576, CADO.)

10. Eckert, E., and Weise, W.: The Temperature of Unheated Bodies in a High-Speed Gas Stream. NACA TM 1000, 1941.

11. Ellerbrock, Herman H., Jr., and Ziemer, Robert R.: Preliminary Analysis of Problem of Determining Experimental Performance of Air-Cooled Turbine. III - Methods for Determining Power and Efficiency. NACA RM E50E18, 1950.

12. English, Robert E., and Wachtl, William W.: Charts of Thermodynamic Properties of Air and Combustion Products from 300° to 3500° R. NACA TN 2071, 1950.

13. Auyer, E. L.: Basis of Correction of Test Results and Extrapolation to Altitude Conditions for Type I Jet-Propulsion Aircraft Gas Turbines. Bull. No. DF81407, Aircraft Gas Turbine Engrg. Div., Gen. Electric Co., Oct. 1, 1945.

14. Ellerbrock, Herman H., Jr., Wcislo, Chester R., and Dexter, Howard E.: Analysis, Verification, and Application of Equations and Procedures for Design of Exhaust-Pipe Shrouds. NACA TN 1495, 1947.

15. Keenan, Joseph H., and Kaye, Joseph: Thermodynamic Properties of Air. John Wiley & Sons, Inc., 1945.

TABLE I – SUMMARY OF ENGINE OPERATING CONDITIONS

Series	Nominal engine speed, N (rpm)	Average compressor-inlet condition		Thermocouple group	Combustion-gas flow w_g (lb/sec)	Fuel flow w_F (lb/sec)	Cooling-air flow per blade w_a (lb/sec)	Cooling-air inlet temperature $T_{a,H}$ (°F)	Cooling-air temperature at blade root $T_{a,e,h}$ (°F)	Calculated turbine-inlet total temperature $T'_{g,S,I}$ (°F)
		Pressure (in. Hg)	Temperature (°F)							
1	4,000	29.2-29.6	36-63	C,I,E,K,F,L	19.7-21.7	0.300-.308	0.011-.175	45-81	50-110	933-1010
2	4,000	29.5	49	A,B,C,D,E,F	19.6-20.7	.292-.299	.008-.148	41-78	50-88	956-962
3	4,000	29.4-29.9	56-70	G,H,I,J,K,L	18.8-19.8	.289-.292	.004-.096	61-82	70-114	1021-1031
4	6,000	29.5-29.8	33-53	A,B,C,D,E,F	32.9-34.5	.417-.421	.006-.105	37-78	50-102	923-968
5	6,000	29.0	62-63	G,H,I,J,K,F	31.5-31.9	.406-.416	.004-.105	56-82	67-119	1005-1010
6	8,000	29.7	47	A,B,C,D,E,F	46.7-47.4	.547-.550	.005-.100	50-66	71-125	997-1005
7	8,000	29.7	47-49	G,H,I,J,K,F	46.9-47.2	.542-.547	.005-.100	48-70	65-123	990-995
8	9,000	29.5-29.7	50-52	A,B,C,D,E,F	52.4-53.7	.639-.642	.006-.106	47-68	80-152	1063-1065
9	9,000	29.2	52-58	G,H,I,J,K,F	51.3-51.9	0.636	.005-.105	57-78	88-166	1085-1090
10	10,000	29.2	57	A,B,C,D,E,F	59.2-59.7	.792-.797	.009-.105	50-70	98-176	1160-1172
11	10,000	29.3	53-63	G,H,I,J,K,F	59.2-59.5	.792-.804	.008-.105	50-69	89-173	1161-1163
12	10,500	29.9	77-81	A,C,D,E,F	59.0-59.6	.881-.884	.010-.105	65-91	108-176	1285-1293
13	10,500	29.1	67	G,H,I,J,K,F	61.2-61.5	.907-.917	.012-.100	57-76	102-191	1278-1280

NACA

TABLE II - PREDICTED ALLOWABLE TURBINE-INLET TEMPERATURES

[Engine speed, 11,500 rpm; cooling-air-flow rate, 5 percent of combustion-gas-flow rate; atmospheric conditions at compressor inlet, standard sea level.]

Blade-fabrication method	Cooling-air temperature $T_{a,e,h}$ (°F)	Allowable turbine-inlet temperature (°F)			
		Timken alloy, 17-22A		High-temperature alloy, X-40	
		Trailing-edge-temperature basis	Midchord-temperature basis	Trailing-edge-temperature basis	Midchord-temperature basis
Shell supporting tubes and base supporting shell	506	1370	2090	1615	2600
	a200	1450	2585	1795	3280
Base supporting shell and tubes	506	1370	2090	1770	2900
	a200	1450	2585	1870	3420

aIntercooler required.

"Page missing from available version"
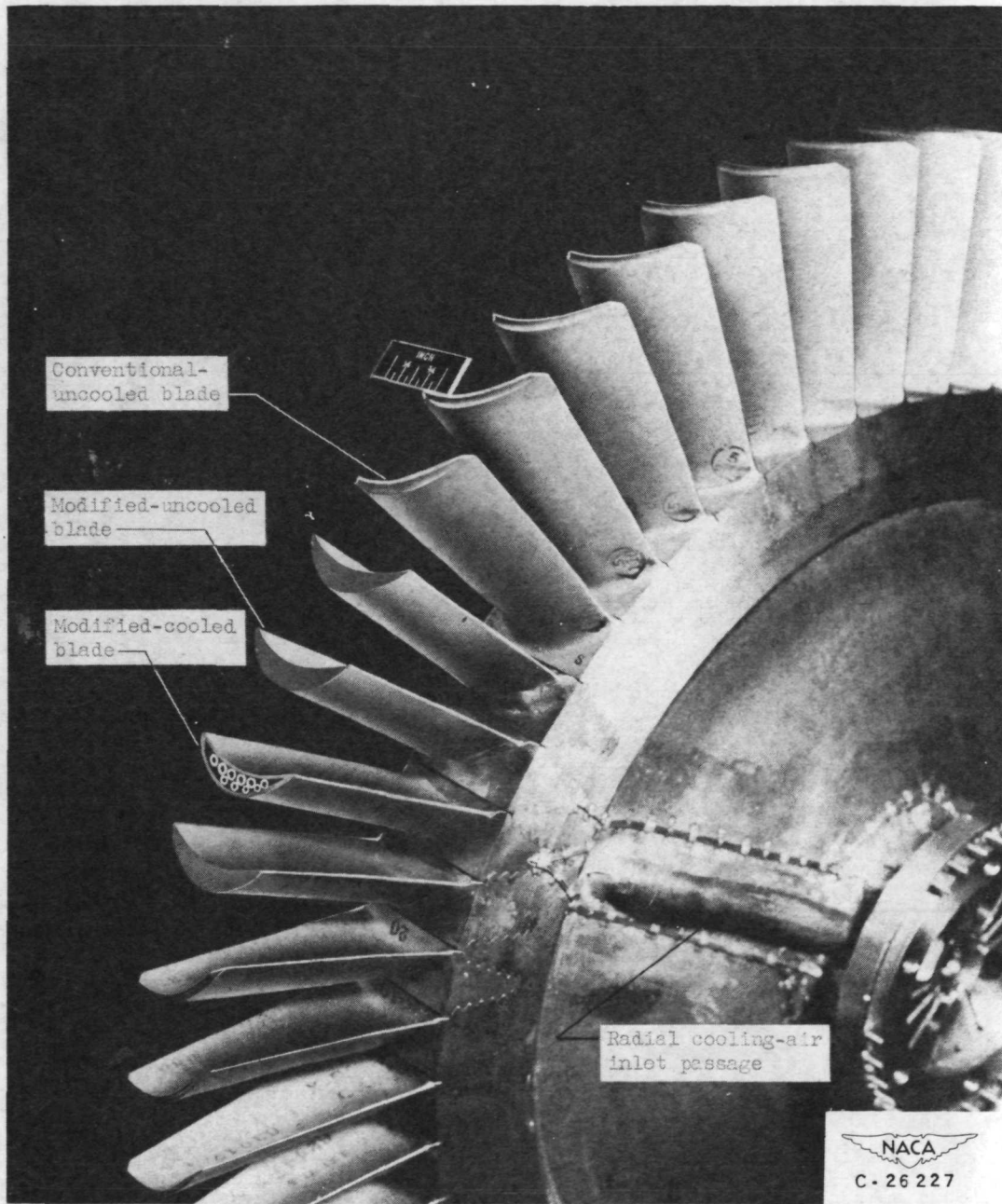
1410

Figure 1 - Modified turbine rotor and blades.

"Page missing from available version"

1410

INCH

Conventional-uncooled
blades

Modified-uncooled blades

Modified-cooled blade
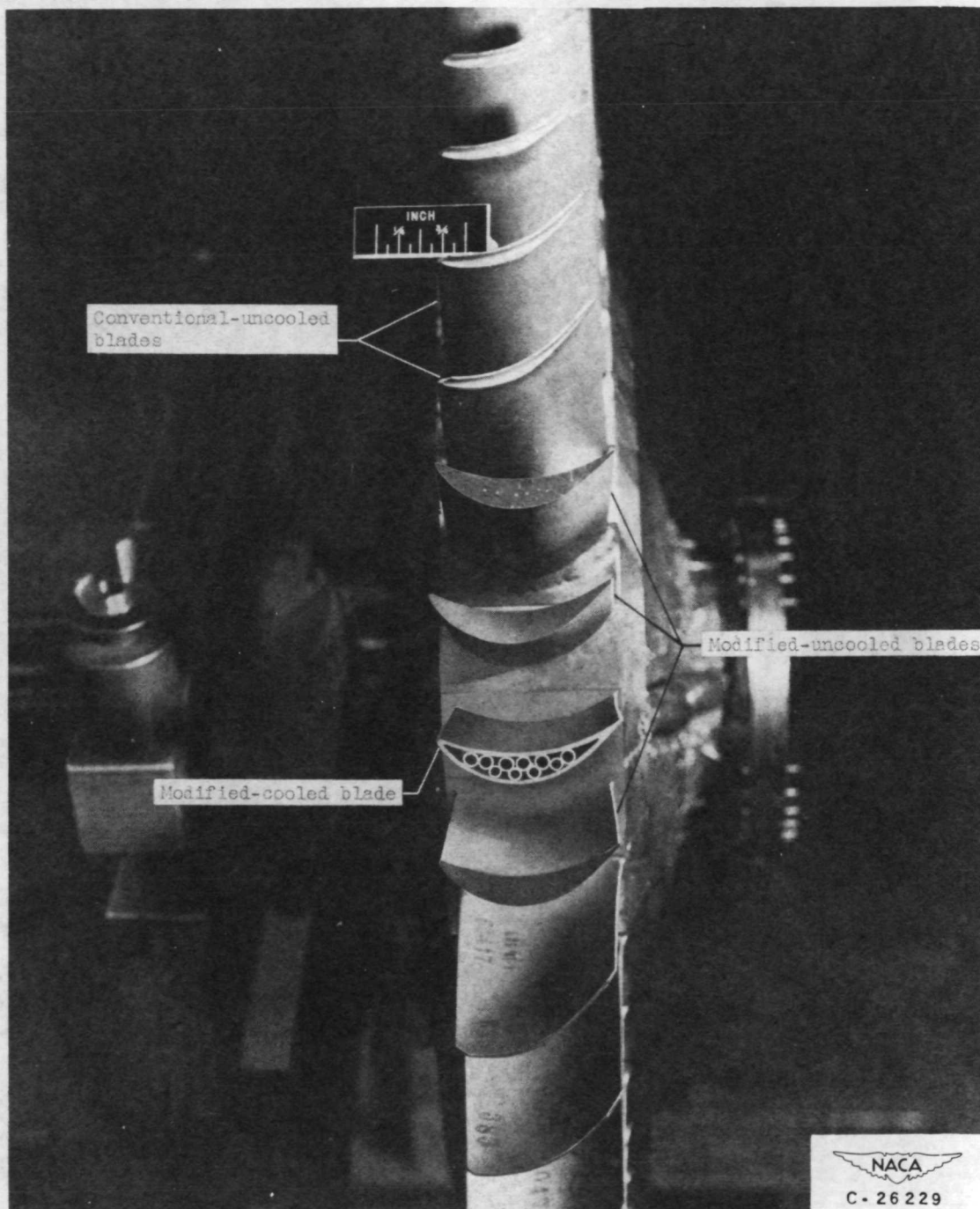
NACA
C-26229

Figure 2. - Top view of modified-blading installation.

"Page missing from available version"
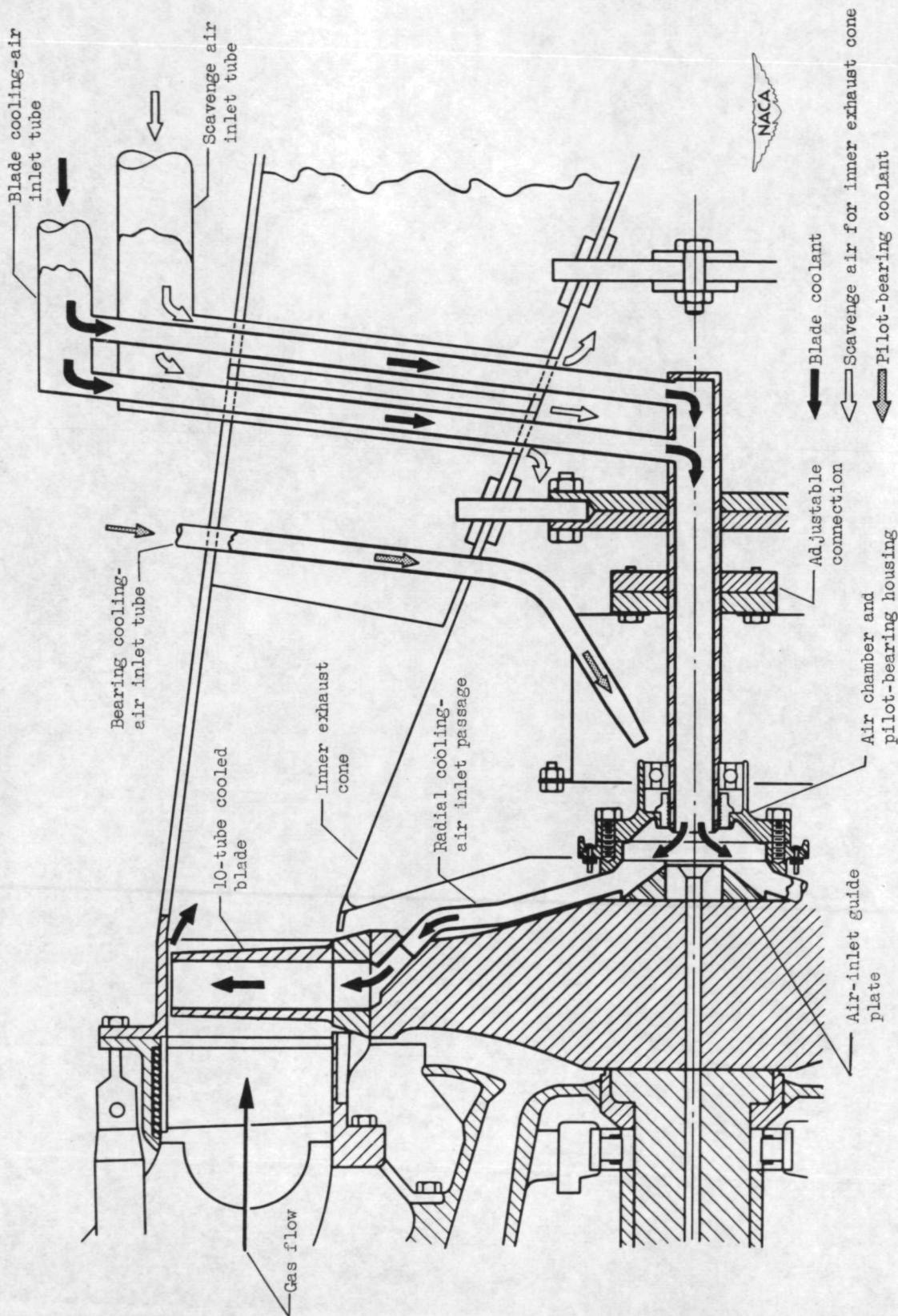
Figure 3. - Modified tail-cone assembly.

"Page missing from available version"

1410

Thermocouple H

Cooling-air slot

NACA
C-26230

(c) Base view of blade.

Thermocouple I

Thermocouple J
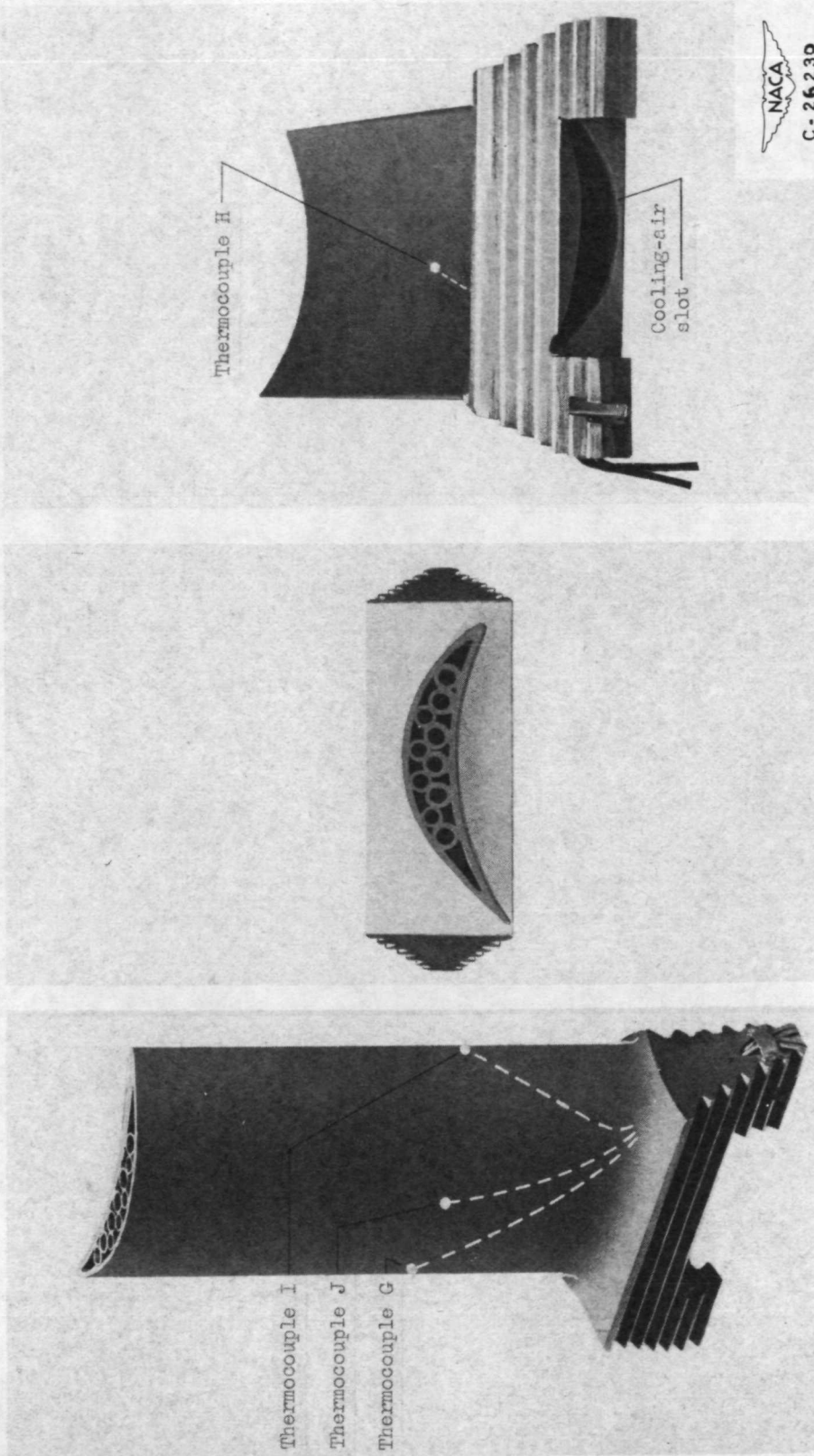
Thermocouple G

(a) Side view of blade.

(b) Tip view of blade.

Figure 4. - Cooled turbine blade.

"Page missing from available version"
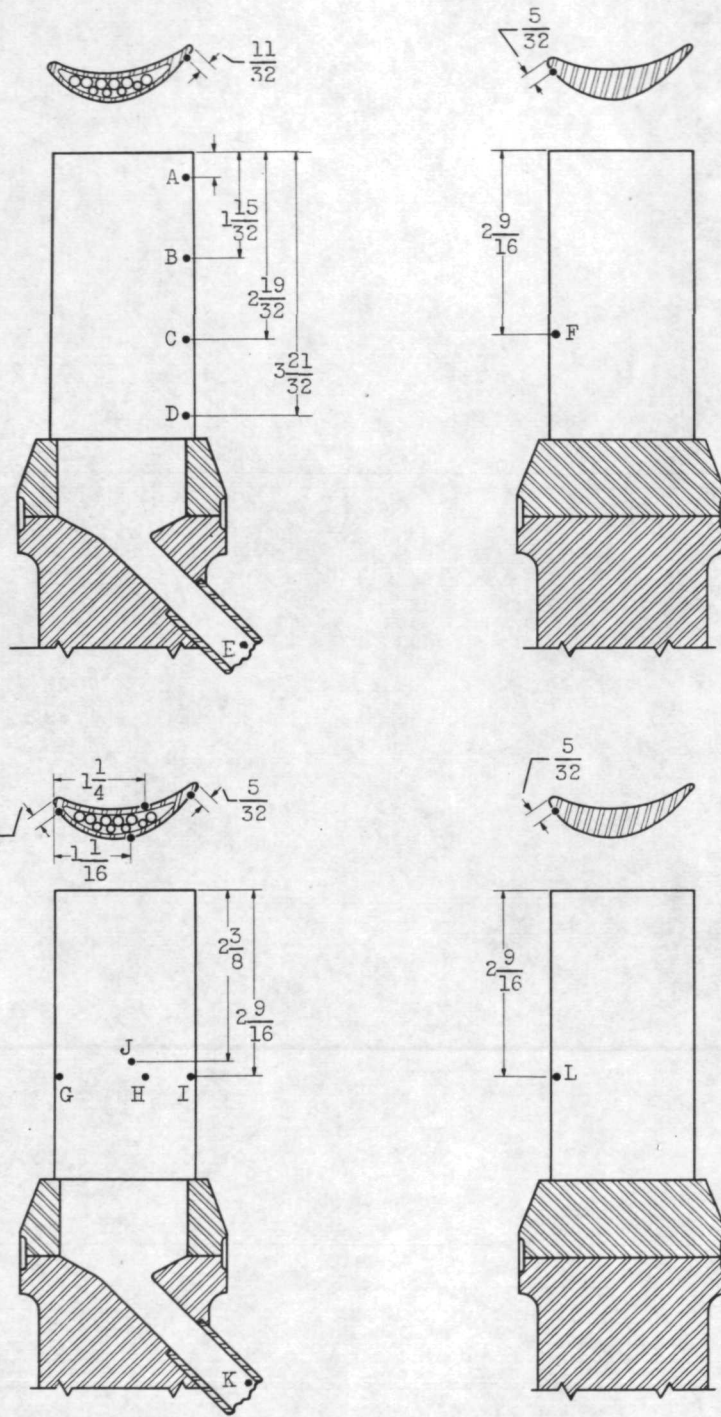
Figure 5. - Turbine-blade thermocouple locations. (All dimensions are in inches.)

"Page missing from available version"
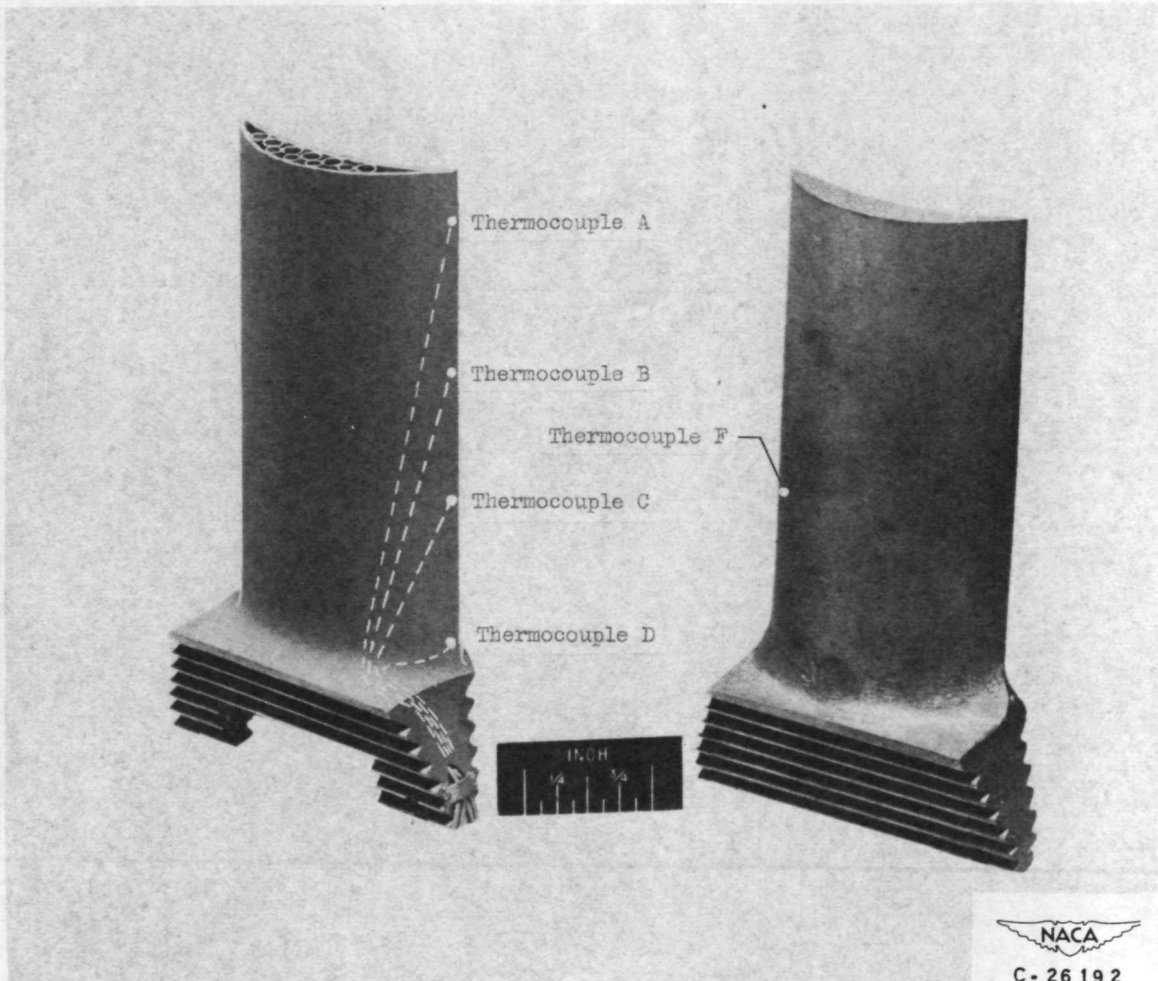
1410

(a) Cooled blade.   (b) Uncooled blade.

Figure 6. - Thermocouple installation on cooled and uncooled blades.

"Page missing from available version"

1410

Bakelite terminal coupling

Thermocouple slip-ring assembly

Cold-junction steam box

NACA
C-26228
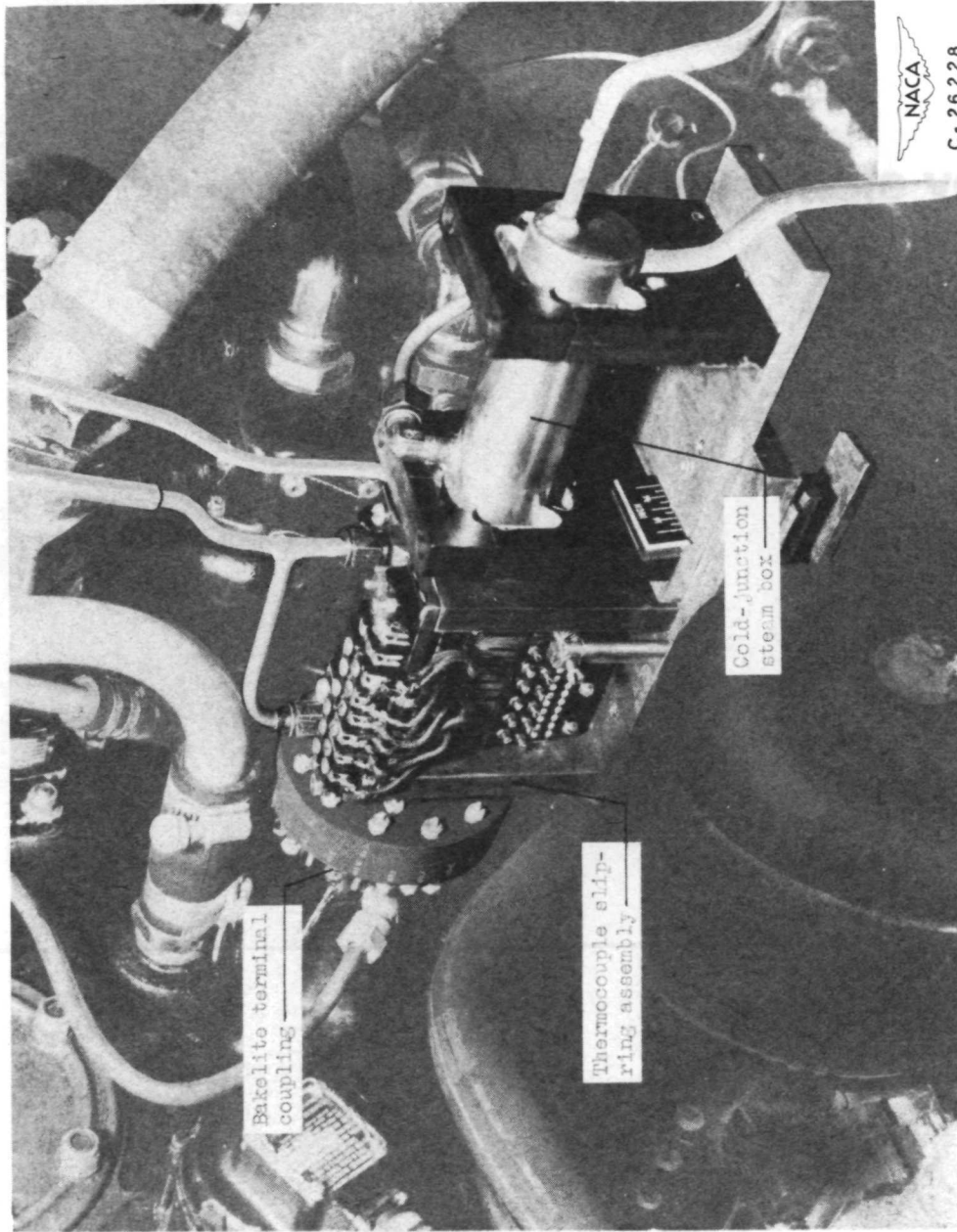
Figure 7. - Thermocouple slip-ring assembly shown mounted on front of engine.
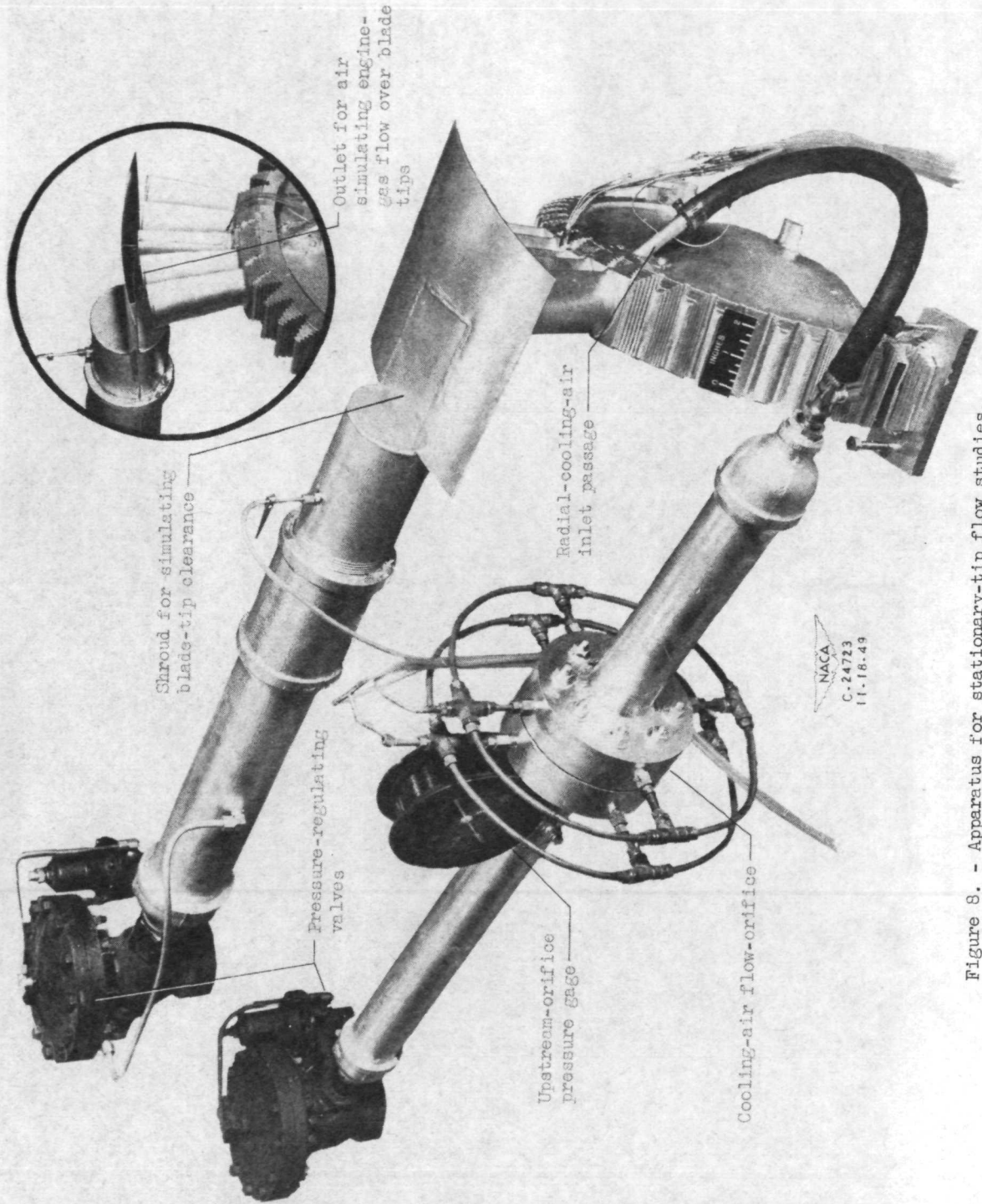
1410

Figure 8. - Apparatus for stationary-tip flow studies.

"Page missing from available version"
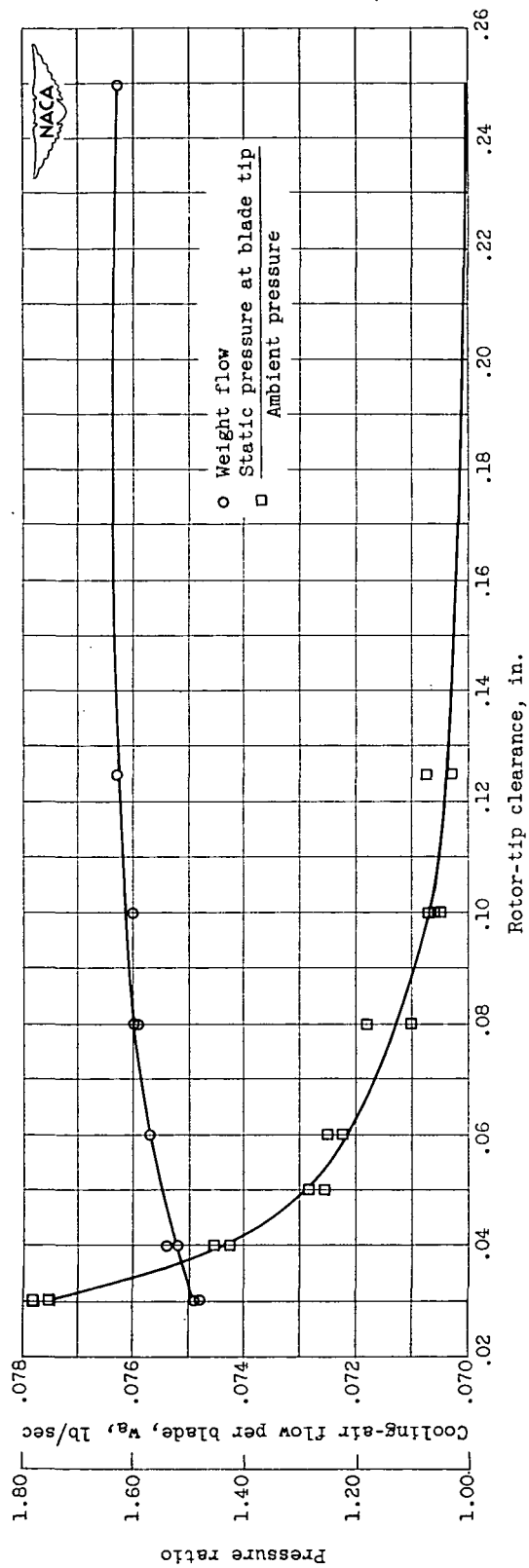
Figure 9. - Effect of rotor-tip clearance on cooling-air flow and ratio of tip pressure to ambient pressure.
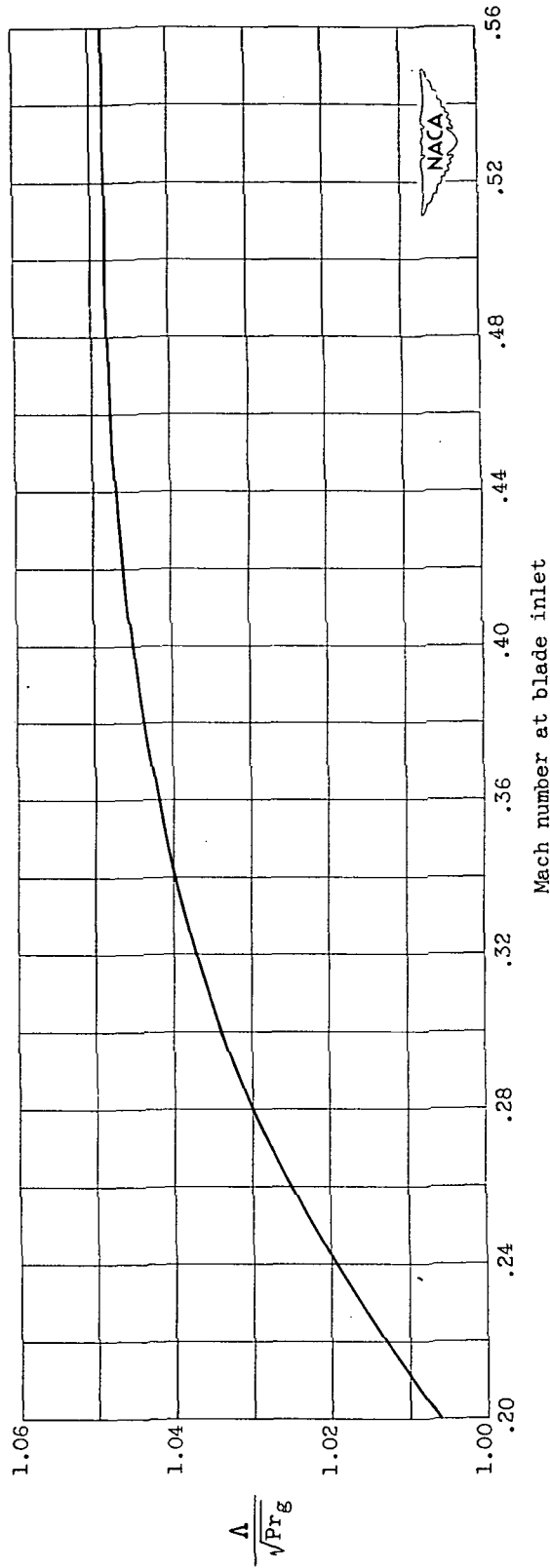
Figure 10. - Recovery factors for Lucite blades in cascade.

1410

(a) Cooling-air temperatures.

(b) Blade temperatures.
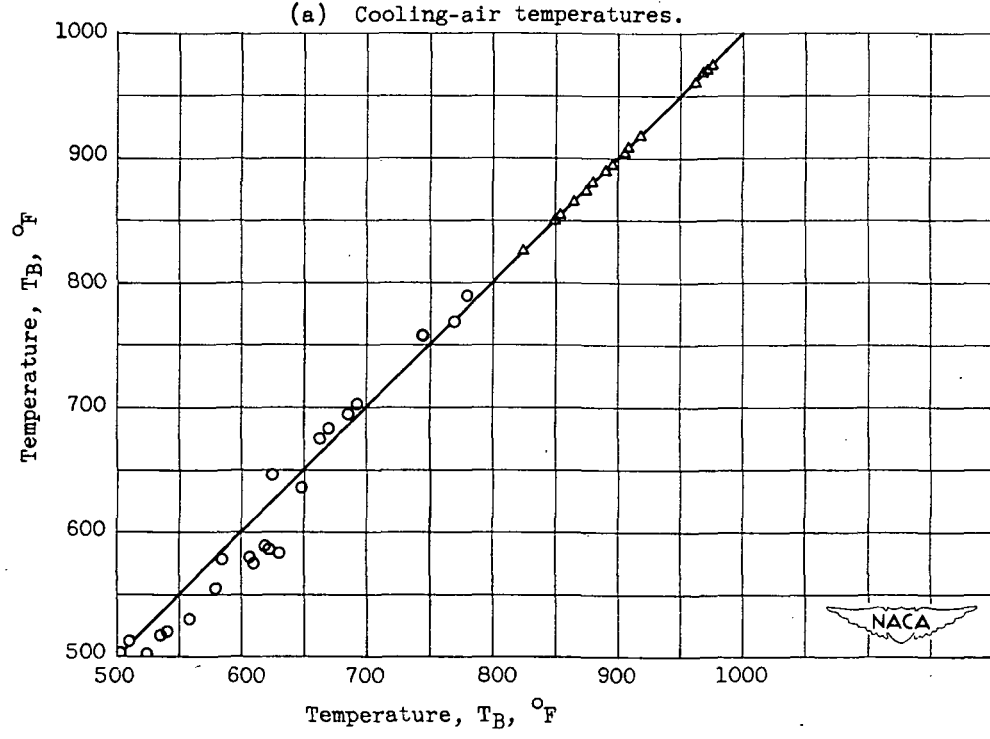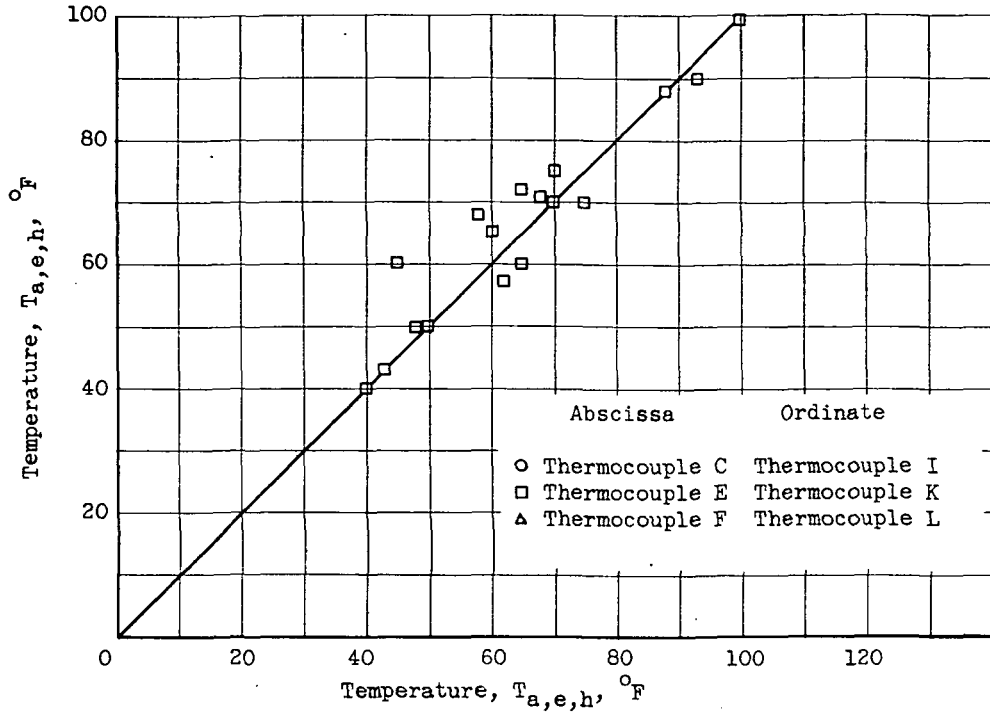
Figure 11. - Temperature comparisons at similar locations for
coolant and blades.
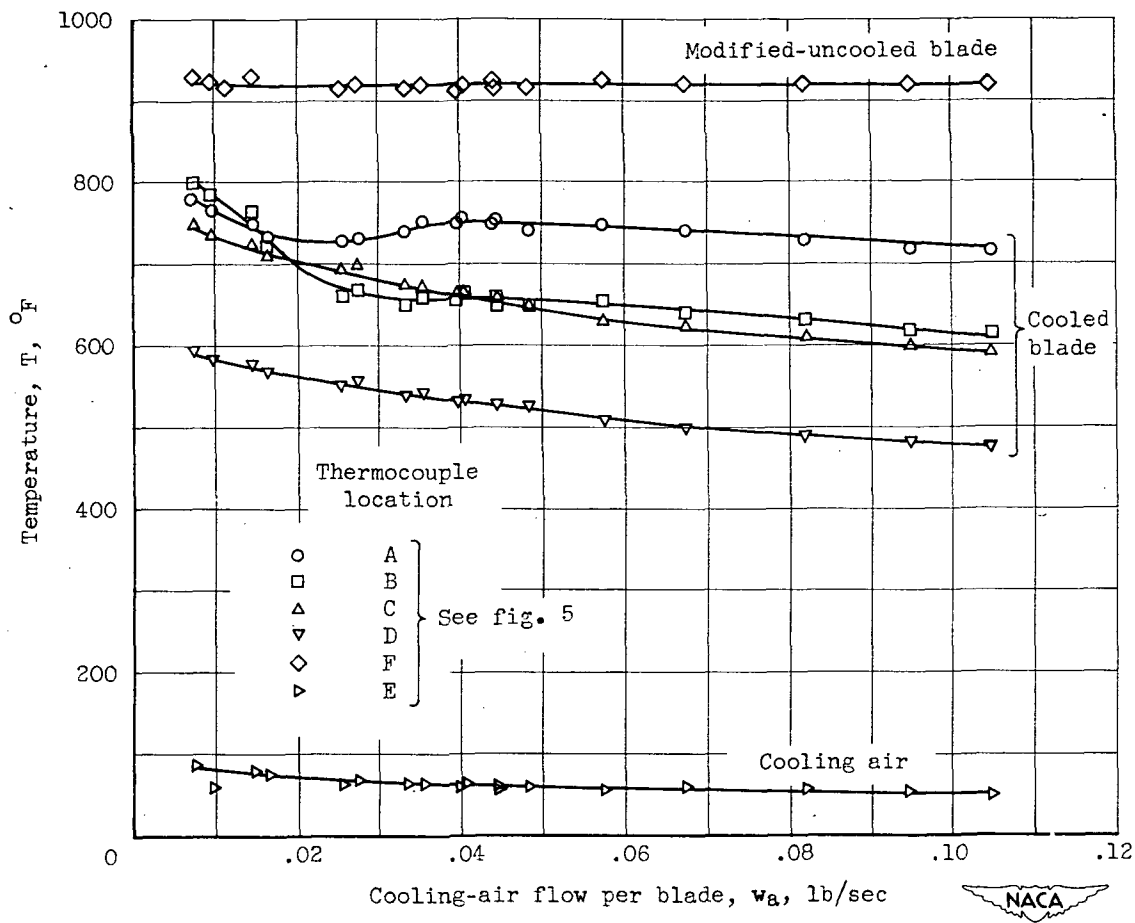
(a) Series, 2; engine speed, 4000 rpm.

Figure 12. - Effect of cooling-air flow on modified blades and cooling-air temperatures.

1410
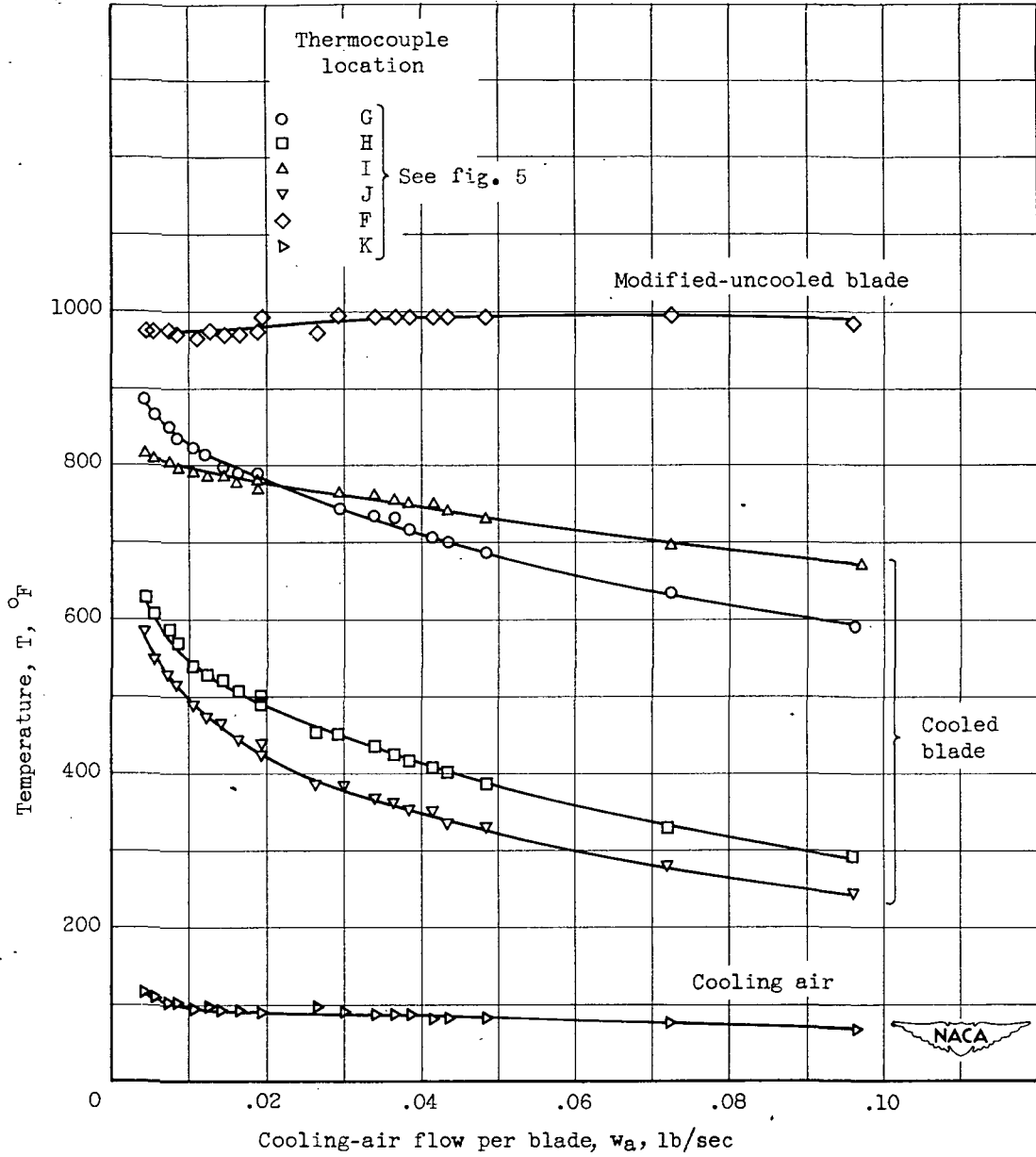
(b) Series, 3; engine speed, 4000 rpm.

Figure 12. - Continued. Effect of cooling-air-flow rate on modified
blades and cooling-air temperatures.
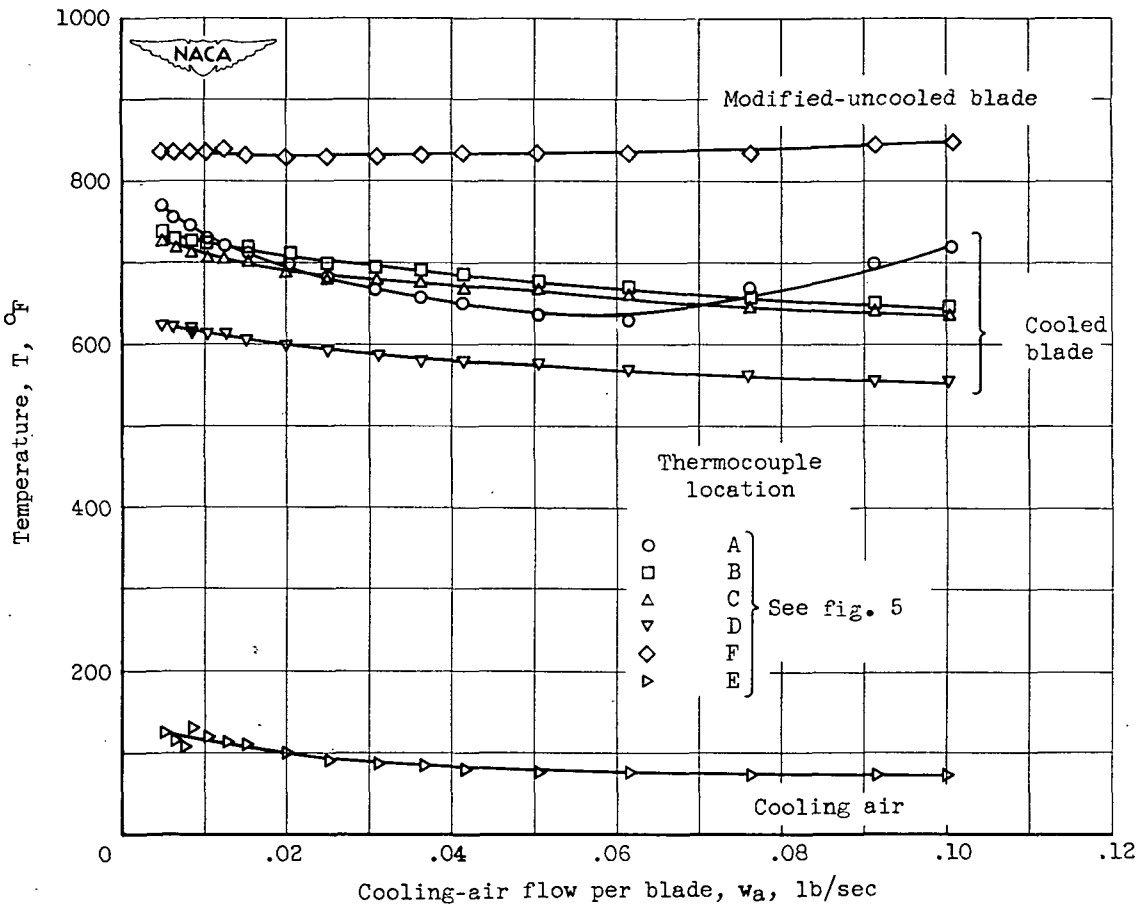
(c) Series, 6; engine speed, 8000 rpm.

Figure 12. - Continued. Effect of cooling-air-flow rate on modified
blades and cooling-air temperatures.

1410
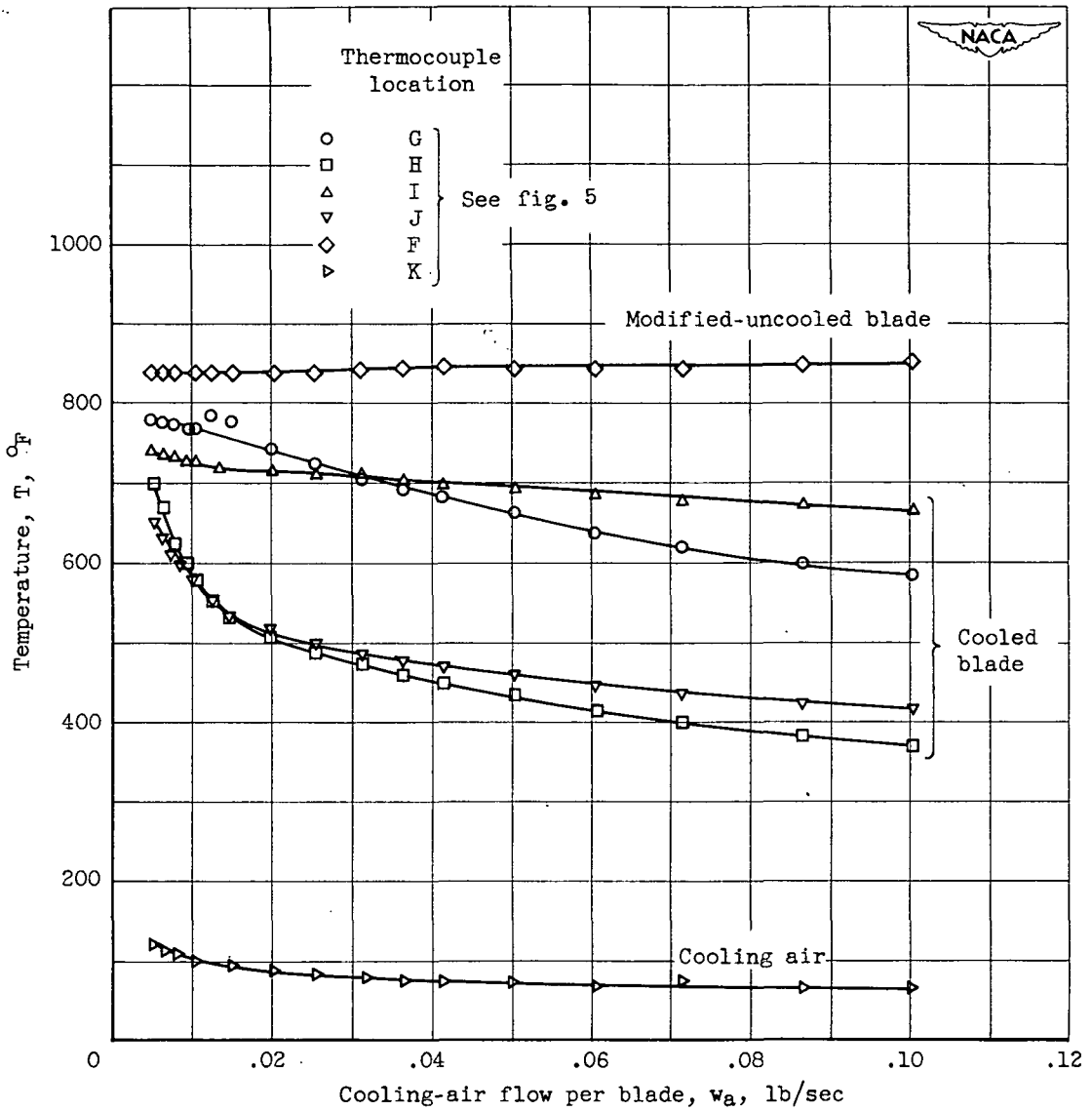
(d) Series, 7; engine speed, 8000 rpm.

Figure 12. - Continued. Effect of cooling-air-flow rate on modified
blades and cooling-air temperatures.
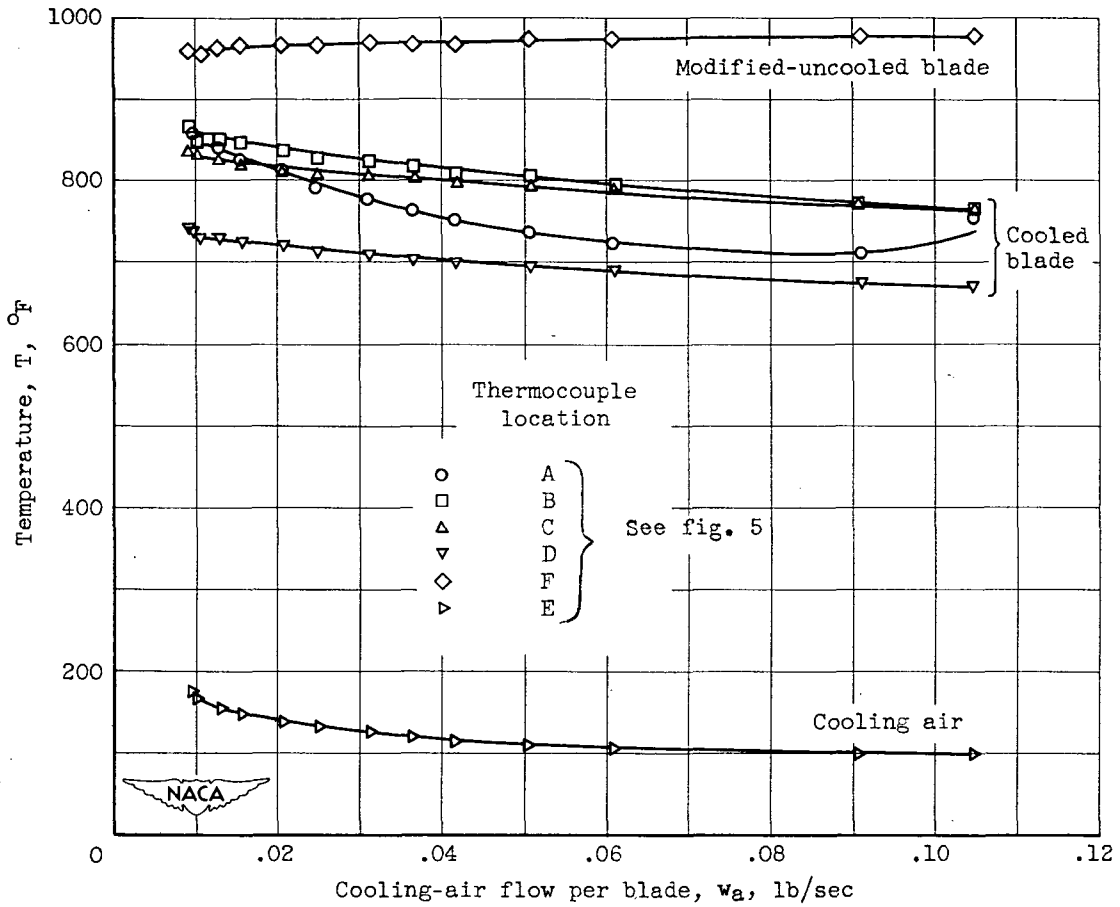
1410

(e) Series, 10; engine speed, 10,000 rpm.

Figure 12. - Continued. Effect of cooling-air-flow rate on modified
blades and cooling-air temperatures.

1410
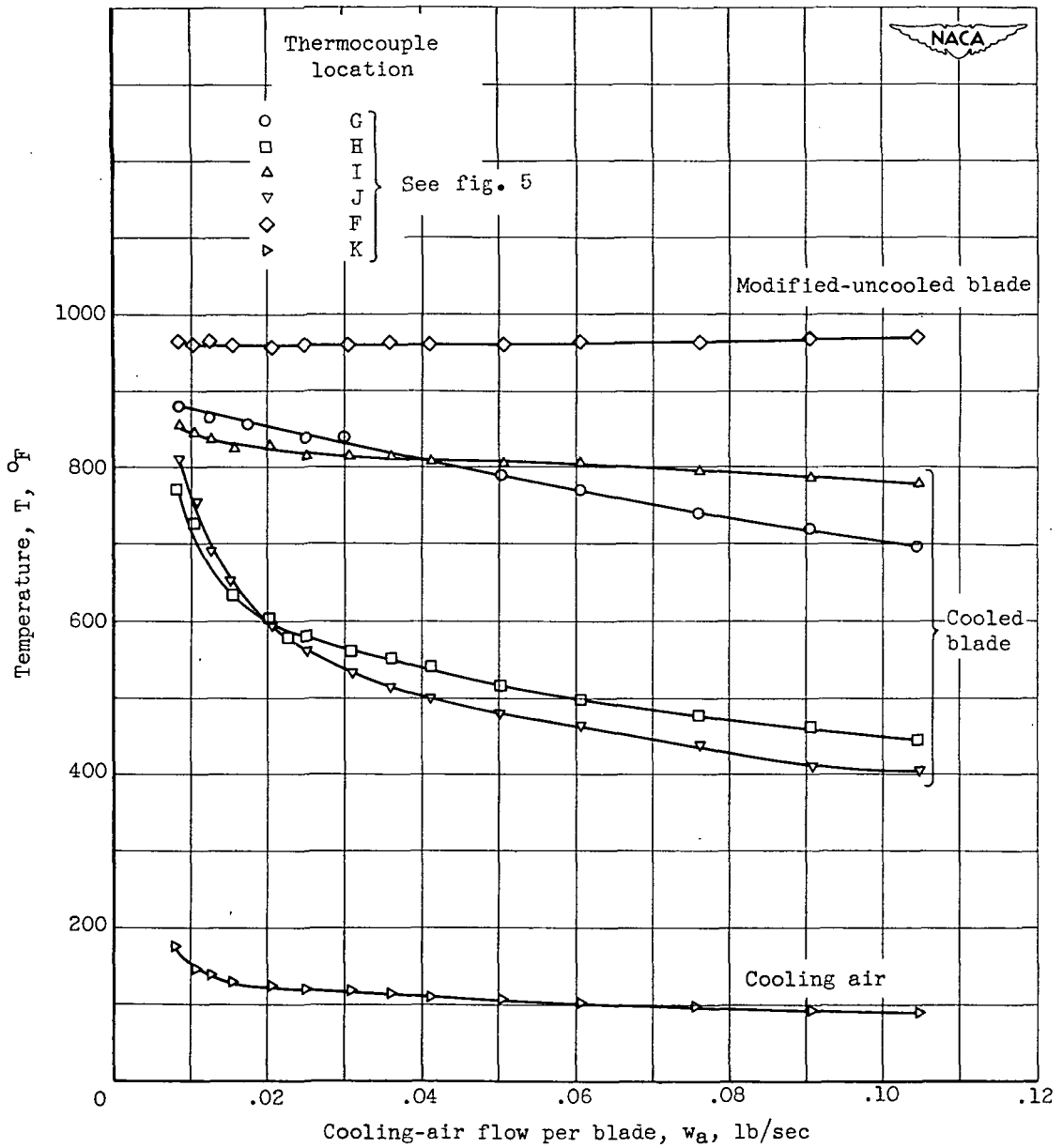
(f) Series, 11; engine speed, 10,000 rpm.

Figure 12. - Concluded. Effect of cooling-air-flow rate on modified
blades and cooling-air temperatures
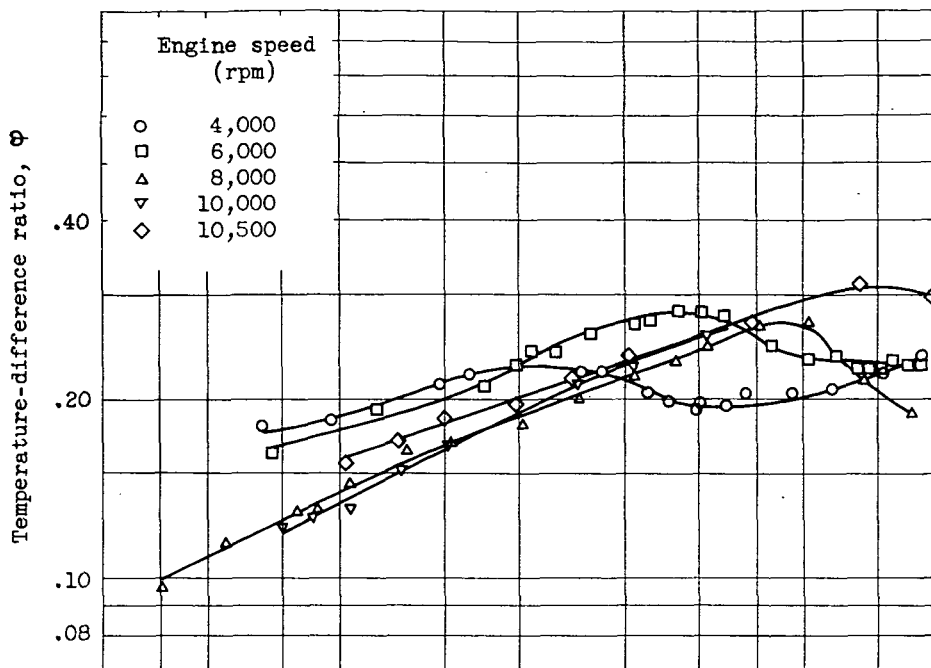
(a) Thermocouple A.
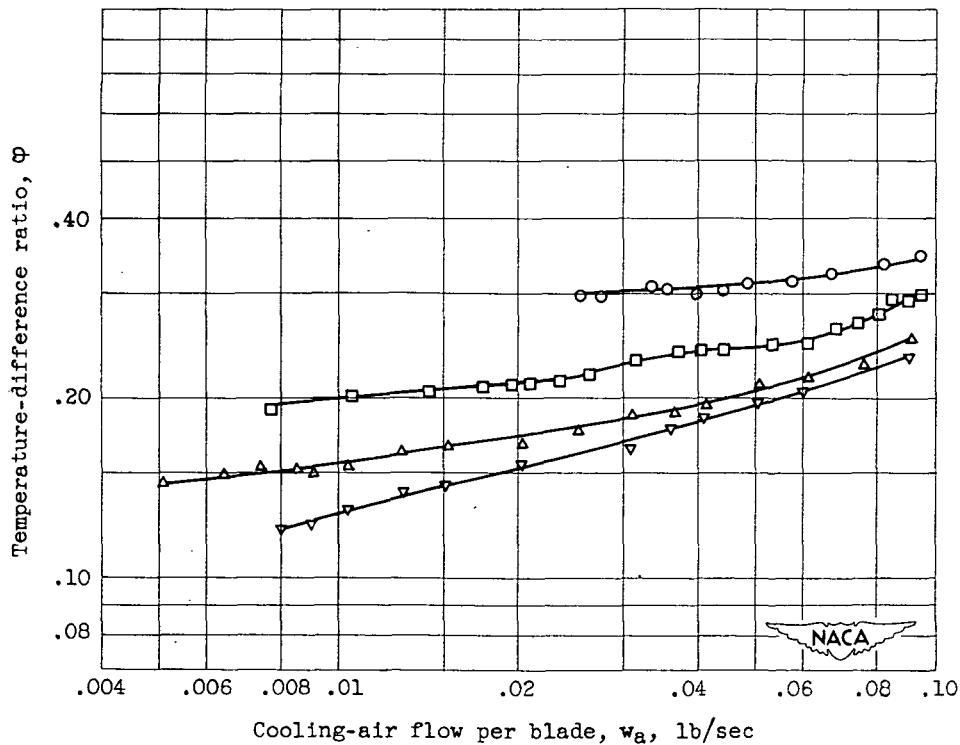
(b) Thermocouple B.

Figure 13. - Effect of cooling-air flow on temperature-
difference ratio for several engine speeds.

1410
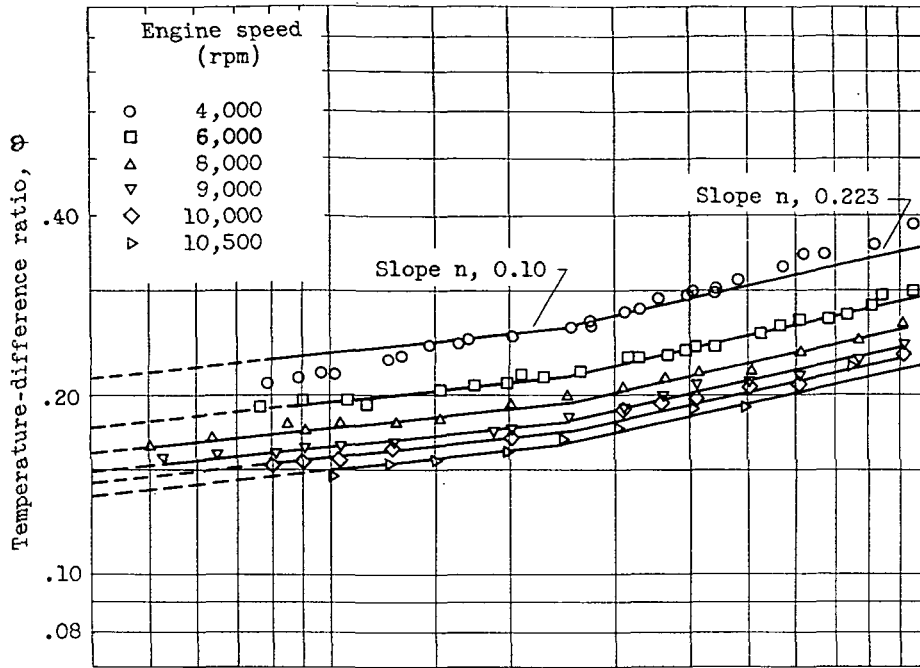
(c) Thermocouple C.
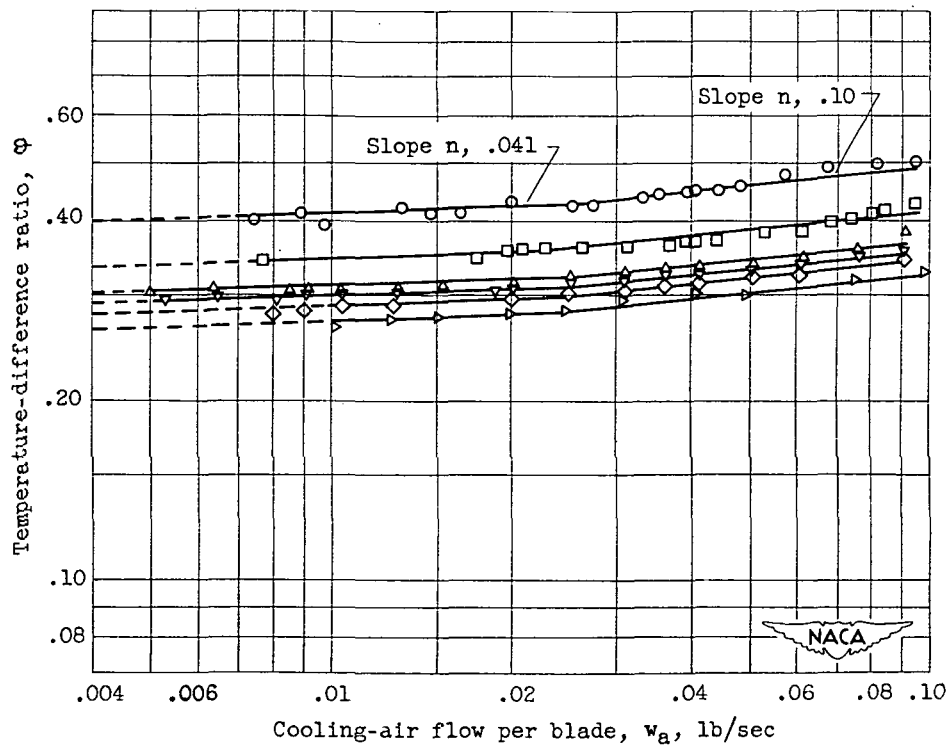
(d) Thermocouple D.

Figure 13. - Continued. Effect of cooling-air flow on temperature
difference ratio for several engine speeds.
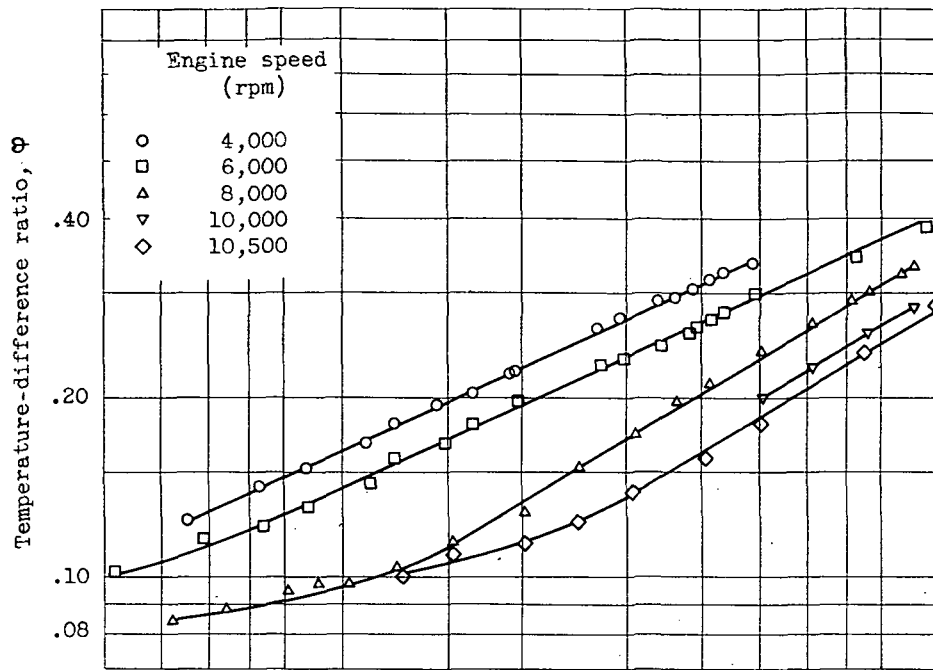
(e)   Thermocouple G.
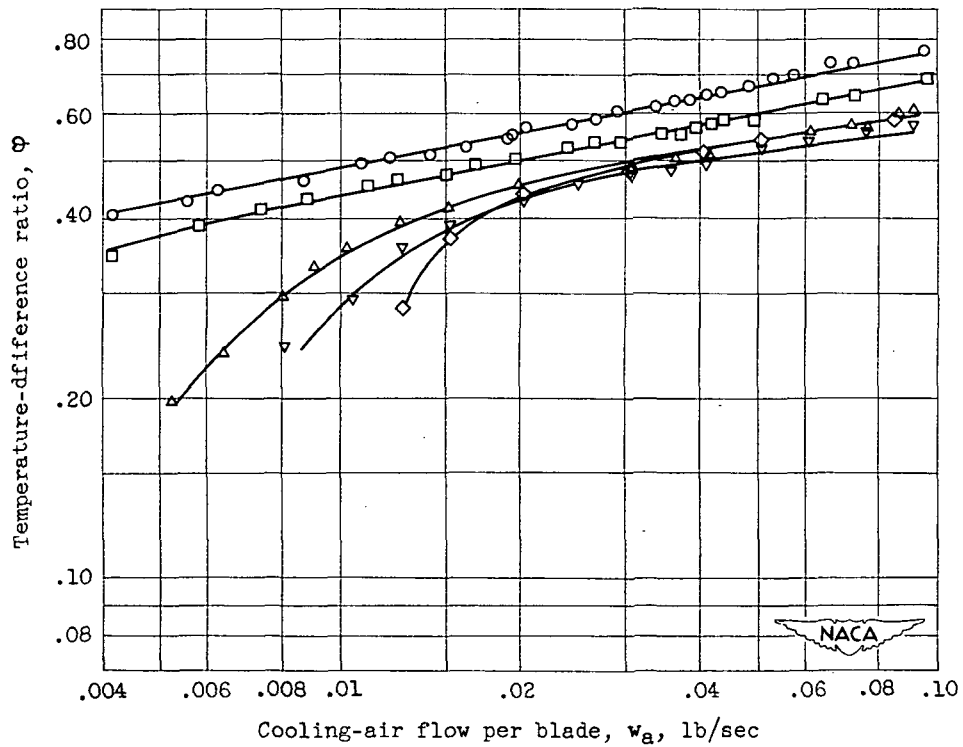
(f)   Thermocouple H.

Figure 13. - Continued. Effect of cooling-air flow on temperature
difference ratio for several engine speeds.
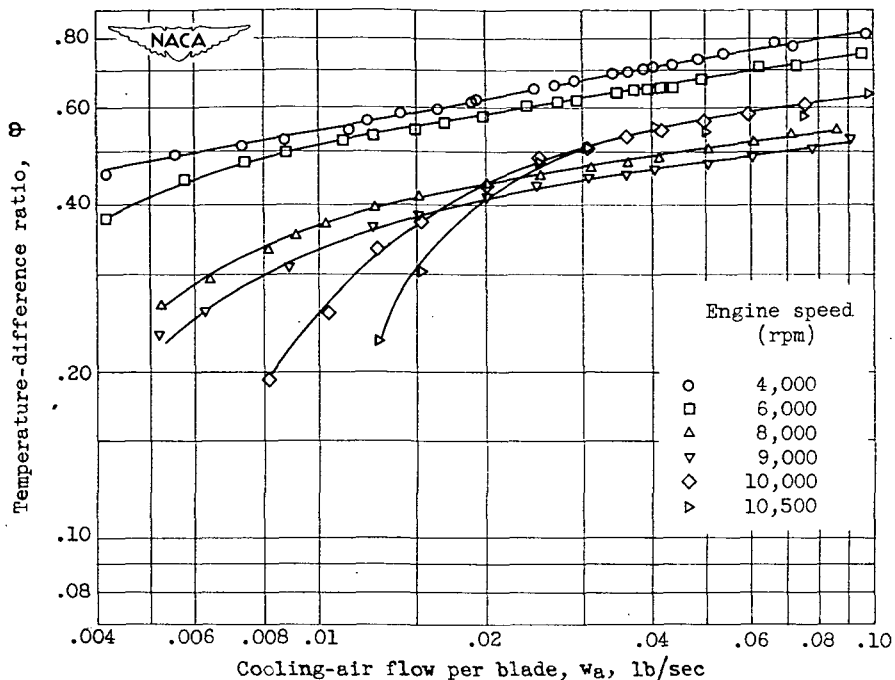
(g) Thermocouple J.

Figure 13. - Concluded. Effect of cooling-air flow on temperature-
difference ratio for several engine speeds.
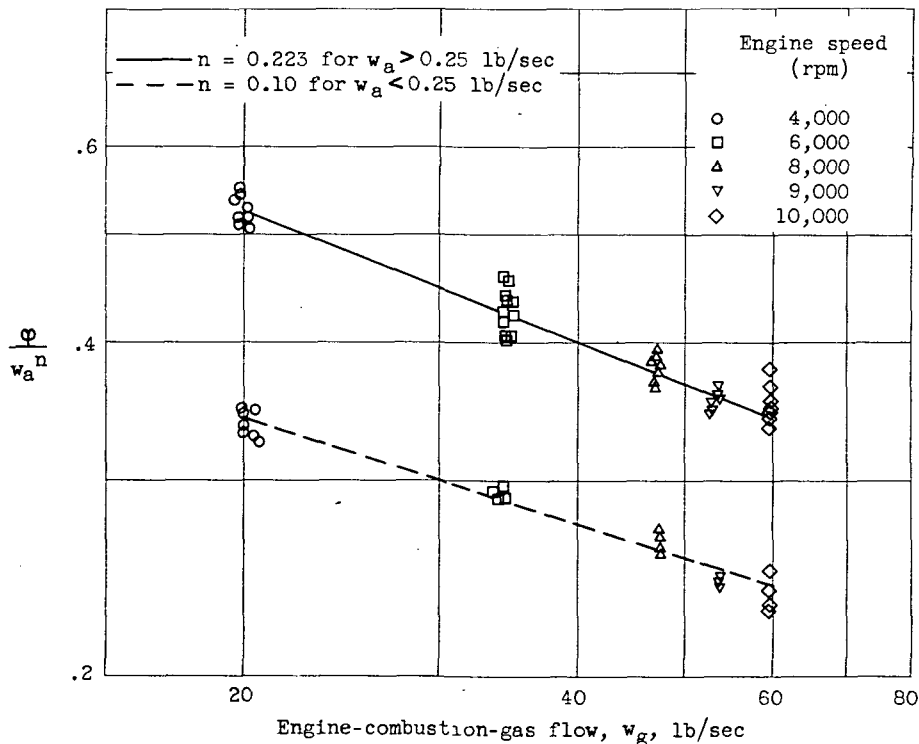
Figure 14. - Variation of φ/w_a^n with engine-combustion-gas
flow for thermocouple C.
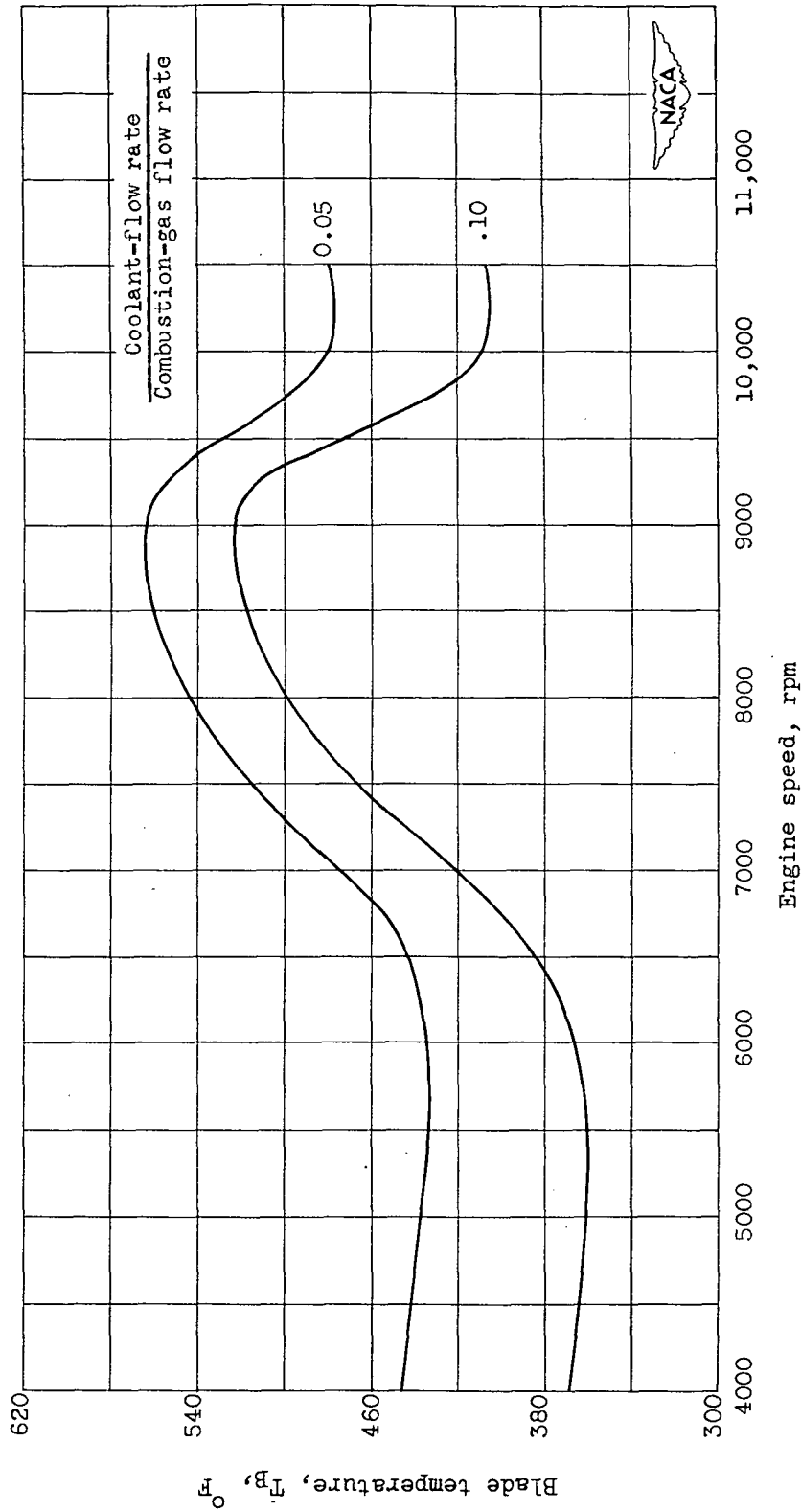
Figure 15. - Variation of cooled-blade temperature at midchord of blade (thermocouple J) with engine speed.

1410
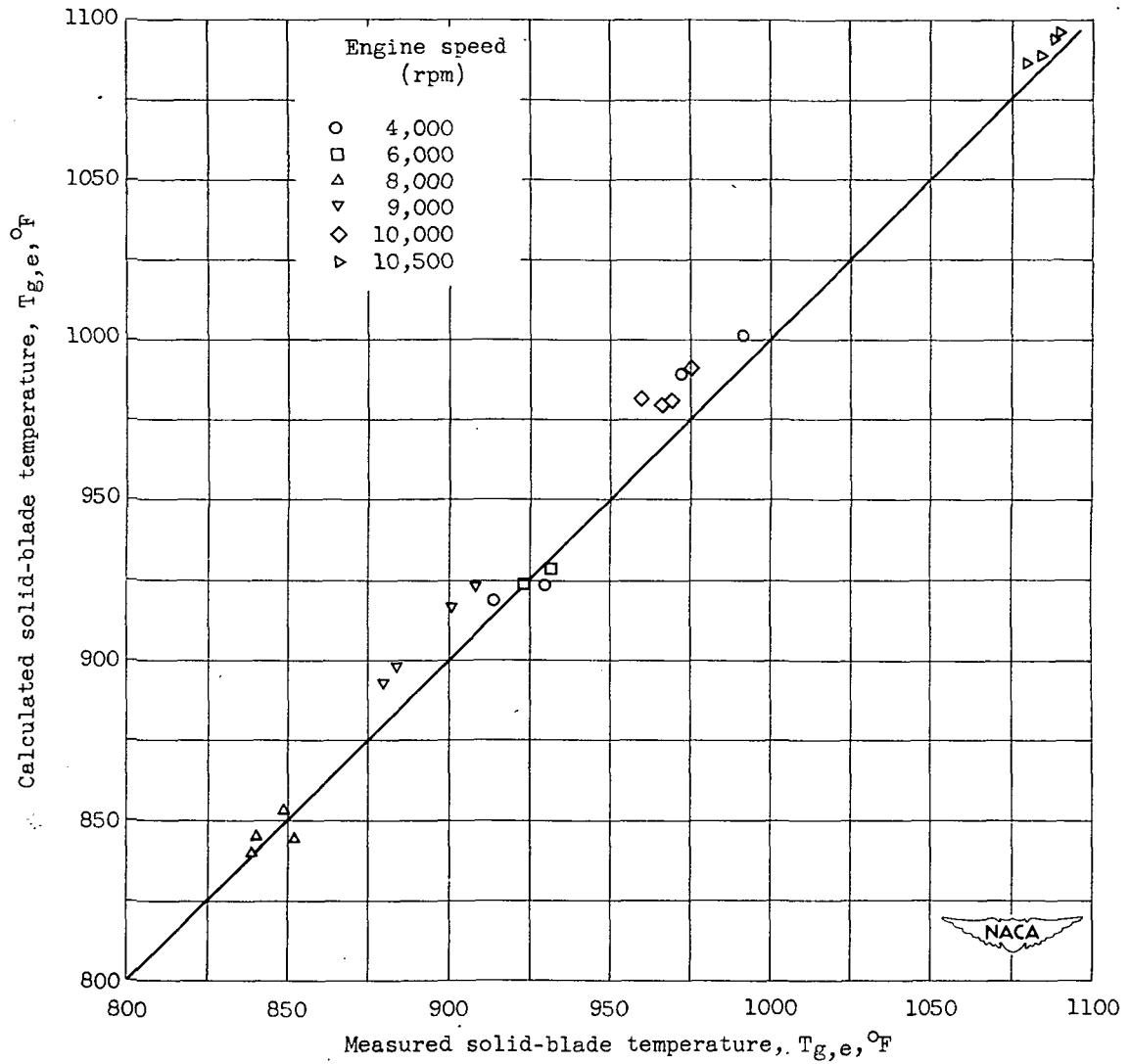
Figure 16. - Comparison of measured solid-blade temperatures with calculated solid-blade temperatures.
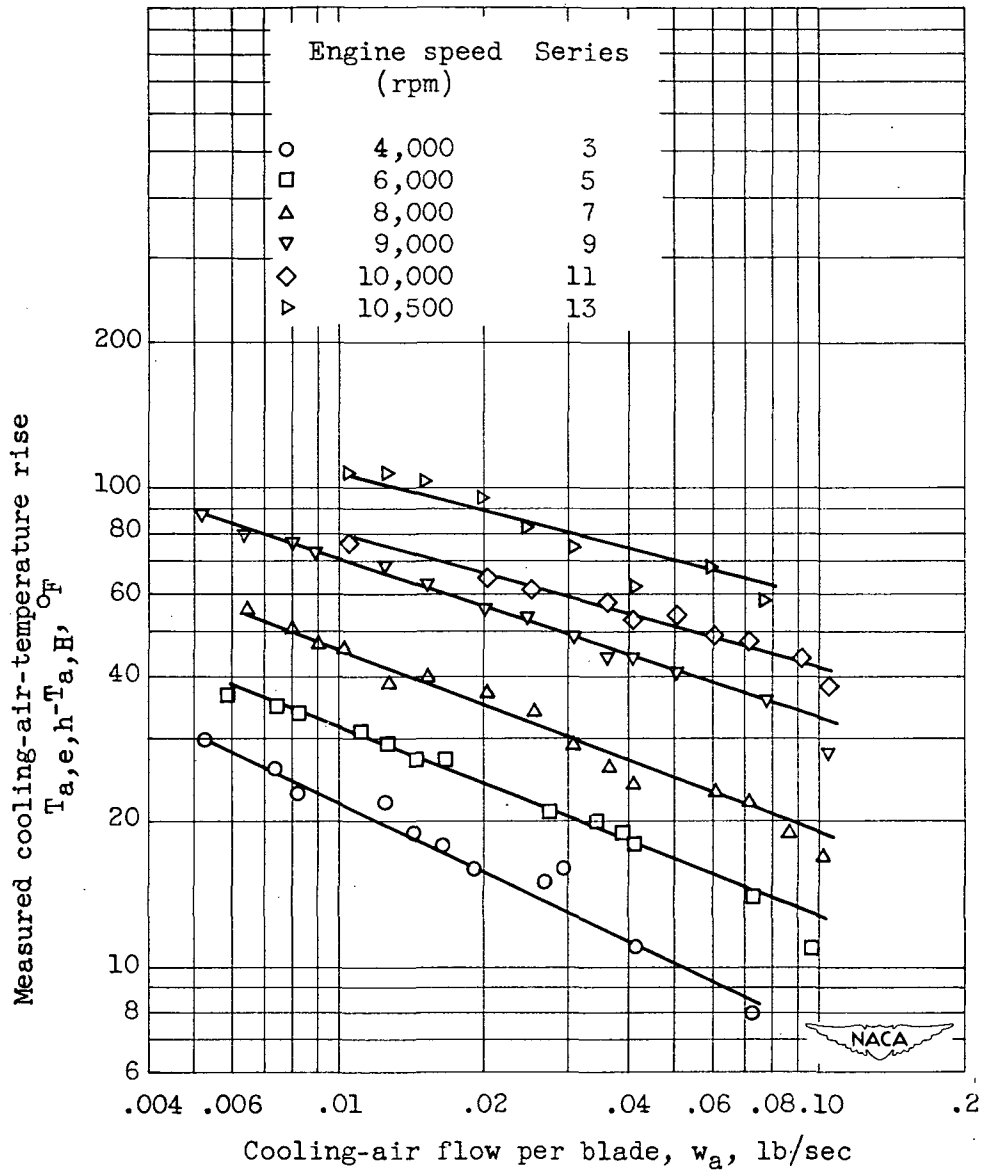
Figure 17. - Effect of cooling-air flow on measured
cooling-air temperature increase from inlet to
blade root at several constant engine speeds.

1410
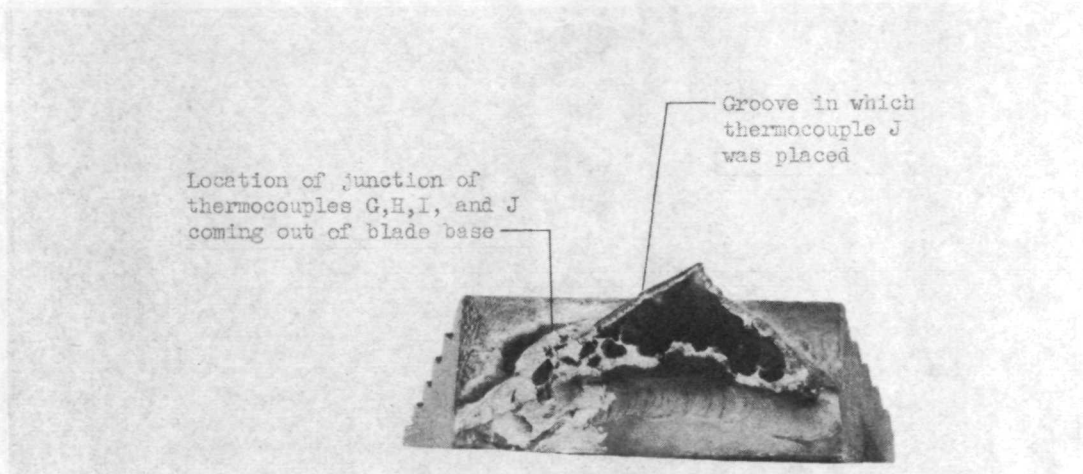
(a) Top view
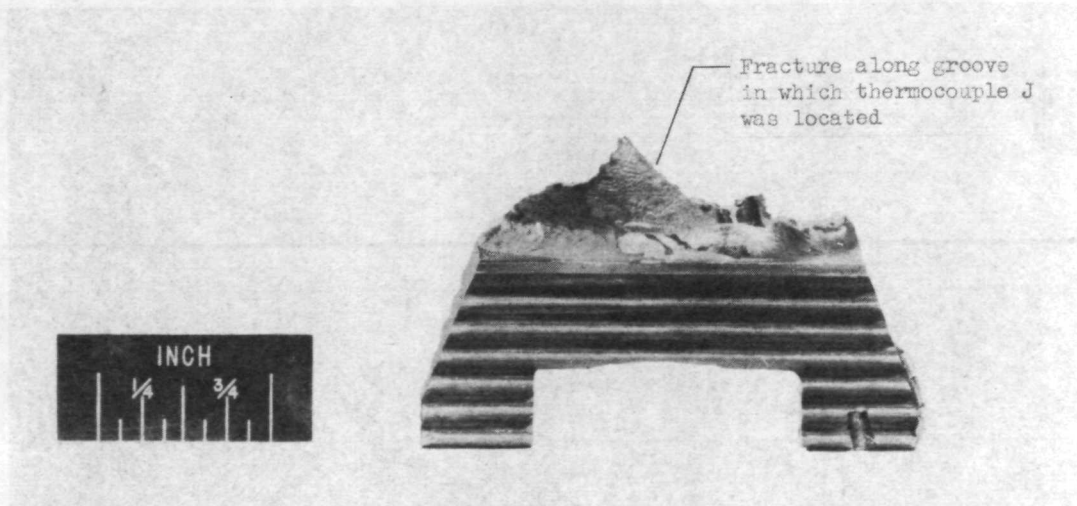
(b) Side view.

Figure 18. - Failure path along fractured blade.

C-25601

"Page missing from available version"
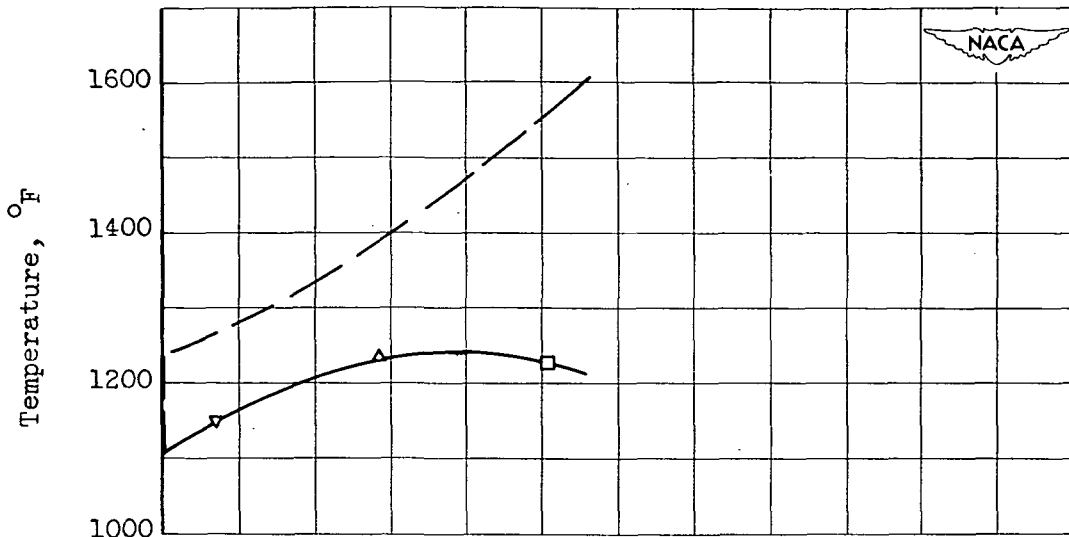
(a)   Blade with tube insert supported by shell.

Distance from blade base, in.
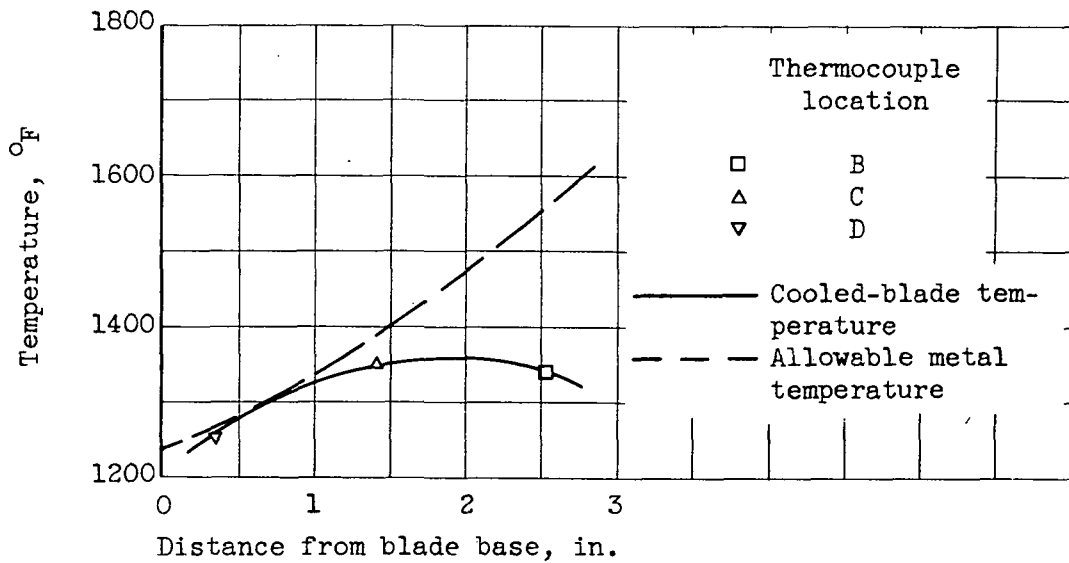
(b)   Blade with tubes supported by base.

Figure 19. - Typical allowable metal and cooled-blade
temperature-distribution curves for engine speed of
11,500 rpm.
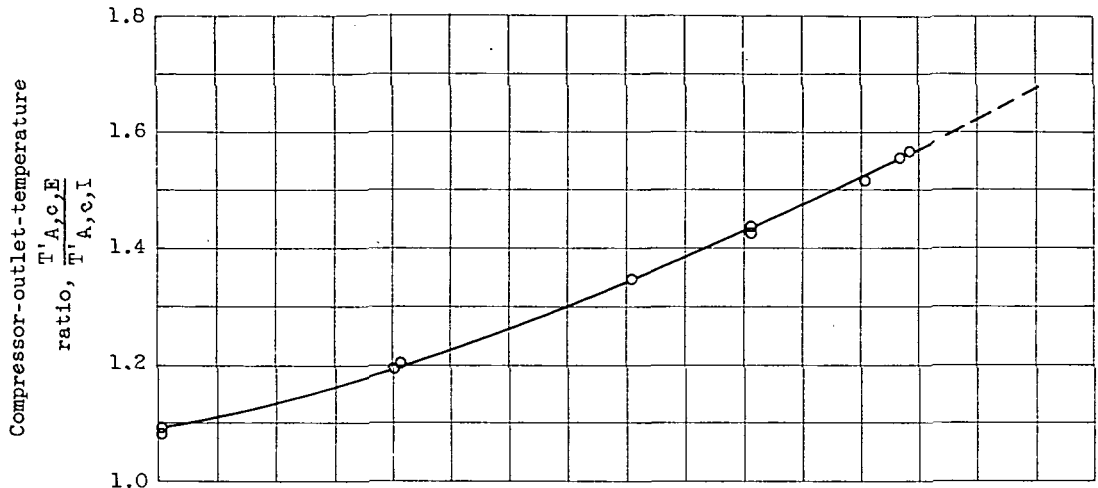
(a)   Compressor temperature ratio
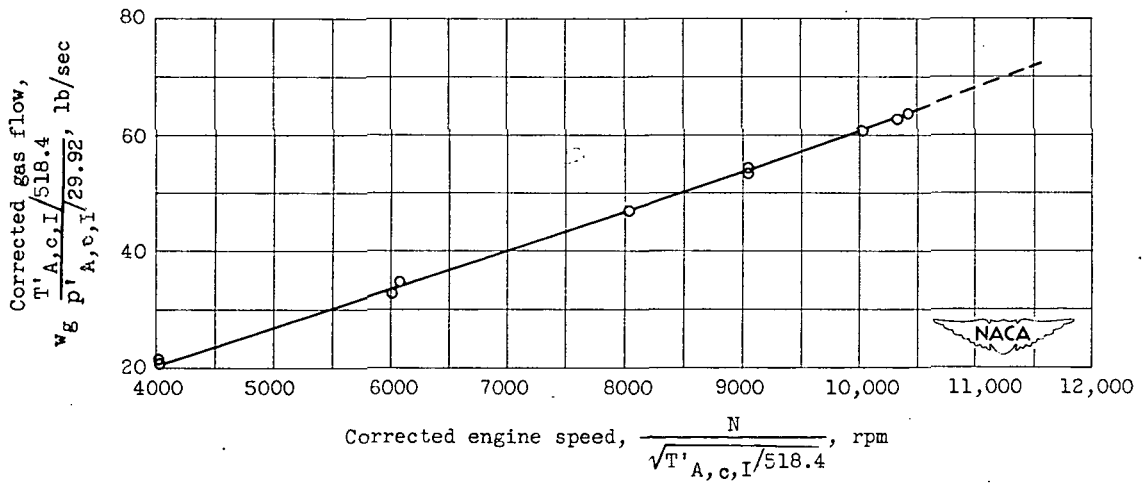
(b)   Corrected gas flow

Figure 20. - Engine operating conditions. (Temperature is given in ^{O}R and pressure in inches of mercury absolute.)